Tomas Bata University in Zlín
Faculty of Technology

Doctoral Thesis Summary

Synthesis of Rotaxane Structures with Multitopic Ligands

Syntéza rotaxanových struktur s vícevazebnými ligandy

Author: **Ing. Aneta Závodná, Ph.D.**

Degree programme: Technologie makromolekulárních látek

Supervisor: doc. Mgr. Robert Vícha, Ph.D.

Consultant: Ing. Zdeňka Prucková, Ph.D.

External examiners: Prof. Uwe Pischel
Prof. Pavel Lhoták

Zlín, February 2025

Published by **Tomas Bata University in Zlín** in the Edition **Doctoral Thesis Summary.**
The publication was issued in the year 2025.

Klíčová slova: rotaxan, supramolekulární chemie, molekulární přepínač, molekulární signál, alosterická aktivace, multitopické ligandy

Keywords: rotaxane, supramolecular chemistry, molecular switch, molecular signal, allosteric activation, multitopic ligands

Full text of the doctoral thesis is available in the Library of TBU Zlín.

"We make our world significant by the courage of our questions and the depth of our answers."

– Carl Sagan, Cosmos

ISBN 978-80-7678-323-2

Abstract

Molecular switches are of considerable interest due to their potential applications in a wide range of fields, including electronics, sensing or medicine. Rotaxanes, i.e., mechanically interlocked molecules, consisting of a ring-shaped molecule (macrocycle) threaded onto an axle-like molecule (thread), can act as molecular switches in certain cases. Both rotaxane components are kinetically trapped as the bulky groups at both ends of the thread are usually larger than the internal diameter of the macrocycle, and therefore this complex cannot undergo dissociation. Rotaxanes can be also considered as a storage of their ring component, which expands their application potential as a complement to the systems that retain the mechanically interlocked manner. In our work, we designed three generations of ligands for the formation of cucurbit[6]uril (CB6) based rotaxane systems, whose axes are equipped with an additional high-affinity binding motif for another macrocycles, cucurbit[7]uril (CB7) and β-cyclodextrin (β-CD). First-generation ligands differed in the length of their central binding motif, while terminal motifs for CB6 slippage (isobutyl, IB) and binding of CB7 (1-adamantylmethyl, Ad) remained invariant. The formation of intended rotaxanes was successful only with the ligand featuring a hexyl motif, as the lengths of the others were not ideal for capturing the CB6. Structures representing second-generation ligands carried bulkier neopentyl-derived terminal moiety for CB6 slipping-on. However, these rotaxanes were not prepared either, as the neopentyl motif is too bulky and does not allow the threading of CB6 under any conditions we used. Finally, successfully assembled rotaxanes of the third-generation consisted of an IB end, 1,6-hexanediammonium centre linker and variable Ad-derived terminal moieties. The difference lay in the length of the linker between the Ad cage and the positively charged nitrogen atom (from methylene to phenylenemethyl spacer). By the shortest rotaxane (with methylene linker), this thesis demonstrates that binding of CB7 to the allosteric Ad binding site, significantly increases the energy of the system which is sufficient for the mechanical barrier to be overcome. This means, that the electrostatic repulsion between the portals of the two CB*n* units can be employed to disassemble a rotaxane to its ring and axle components. Moreover, the kinetics of the slipping-off process can be tuned by the length of the allosteric binding site where the CB7 acts (ethylene, propylene, propenylene spacer). Finally, upon liberation from the rotaxane, the CB6 wheel can be utilized in forming complexes with other guests (i.e., spermine) present in the mixture.

Abstrakt

Molekulární přepínače či spínače jsou zajímavé především díky svým potenciálním aplikacím v široké škále oblastí, včetně elektroniky či medicíny. Rotaxany, tedy mechanicky uzamčené molekuly, sestávající z cyklické molekuly navlečené na druhou, lineární molekulu, představující osu systému, se v určitých případech mohou chovat jako molekulární spínače. Obě komponenty rotaxanu jsou vzájemně kineticky zachyceny, jelikož objemné skupiny nacházející se na obou koncích lineární komponenty jsou zpravidla větší než je vnitřní průměr kavity makrocyklu, a proto nemůže tento komplex disociovat. Rotaxany lze také považovat za jakési úložiště jejich cyklické složky, což rozšiřuje jejich potenciál jako doplněk k systémům, které si během funkce zachovávají své mechanické propojení. V naší práci jsme navrhli tři generace ligandů pro tvorbu rotaxanových systémů založených na cucurbit[6]urilu (CB6), jejichž osy jsou vybaveny dodatečným vysoce afinitním vazebným motivem pro další makrocykly, v podobě cucurbit[7]urilu (CB7) a β-cyklodextrinu (β-CD). Ligandy první generace se lišily délkou centrálního vazebného motivu, zatímco koncové motivy pro navléknutí CB6 (isobutyl, IB) a pro komplexaci s CB7 (1-adamantyl, Ad) zůstaly stejné. Příprava zamýšlených rotaxanů byla úspěšná pouze u ligandu s hexylový motivem, jelikož délky ostatních (4C, 8C, 10C) nebyly ideální pro zachycení CB6. Struktury představující ligandy druhé generace nesly objemnější neopentylový terminální motiv navržený pro navlékání CB6. Nicméně, ani příprava těchto rotaxanů nebyla úspěšná, jelikož neopentylový motiv je již příliš objemný a neumožnil navléknutí CB6 na osu za jakýchkoli námi použitých podmínek. A konečně, úspěšně připravené rotaxany třetí generace sestávaly z IB konce, hexan-1,6-diammoniového centrálního motivu a druhého konce odvozeného od adamantanu, kde rozdíl spočíval v délce spojky mezi adamantanovou klecí a kladně nabitým atomem dusíku (od methylu po fenylenmethyl). Tato práce pomocí nejkratšího rotaxanu (s methylenovou spojkou) demonstruje, že navázání CB7 na alosterické vazebné Ad místo významně zvyšuje vnitřní energii systému, která je dostatečná pro překonání mechanické bariéry. To znamená, že elektrostatická repulze mezi portály obou jednotek CB*n* je využita k rozložení rotaxanu na jeho samotnou cyklickou a lineární složku. Jak se ukázalo, tak kinetiku procesu vyvlékání lze ladit délkou alosterického vazebného místa, na které se váže CB7 (ethylenová, propylenová a propenylenová spojka). CB6 pak může být, po „osvobození“ z rotaxanového systému, využit k tvorbě supramolekulárních komplexů s jinými hosty (například sperminem) přítomnými ve směsi.

Content

Introduction

Jean-Marie Lehn in 1996 wrote '*Beyond molecular chemistry based on the covalent bond lies the field of supramolecular chemistry, whose goal it is to gain control over intermolecular bond. It is concerned with the next step in increasing complexity beyond the molecule towards the supermolecule and organized polymolecular systems, held together by noncovalent interactions*.'.[1]

Since the early research work of Professor Lehn, supramolecular chemistry has become a significant multidisciplinary field, linking, and advancing various fundamental disciplines such as chemistry, physics, physical chemistry and biology. Over the years, its principles have emerged in nanotechnologies and polymer and material sciences. The beginnings of supramolecular chemistry can be associated with the selective binding of alkali metal cations using both natural compounds, such as valinomycin, and synthetic macrocyclic and macropolycyclic ligands, crown ethers, and cryptands. This was followed by the discovery of self-assembly in both organic and inorganic systems, where scientists cleverly utilized metal coordination, hydrogen bonding, or donor–acceptor interactions to achieve the spontaneous formation of various new and interestingly sophisticated systems, including rotaxane structures. From the synthesis of the very first mechanically interlocked molecules and the understanding of their uniqueness in how their individual components can influence each other based on external stimuli (such as changes in pH, light, or a chemical impulse), it was only a short step towards development of advanced artificial molecular machines that can find applications in many fields. In terms of applications, these molecular machines can be used for drug delivery systems, the development of molecular catalytical devices, muscles, rotors, sensors, molecular memories or switches. It is therefore not surprising that the interest of our research group, from studying simple host–guest systems where ligands based on cage hydrocarbons act as guests and macrocyclic compounds from the cucurbit[*n*]uril and cyclodextrin families act as hosts, is gradually shifting towards the design and construction of more sophisticated functional advanced molecular systems, i.e. rotaxanes. The area of focus is the study of lateral interactions between macrocyclic compounds that are bound within a single molecule, as these are crucial insights necessary for the design and construction of functional responsive systems.

Rotaxanes can serve as storage devices for their wheel components, which can be released on demand by overcoming mechanical barriers. Unlike synthesis, rotaxane disintegration is less reported[2–11] and usually requires high temperatures and competitors to destabilise the wheel's position. However, ambient-temperature systems have been developed, such as Leigh's pH-dependent removal of crown ether[12] or Li's modulation of slippage speed via conformational changes of H-bonded arylamide foldamers.[13] Indeed, the most frequent method

for releasing a wheel from rotaxane is to destroy an axel or to remove the stopping moiety.[3,14–18]

The story of the rotaxane systems presented in this thesis reaches its peak with the description of a method for releasing cucurbit[6]uril (CB6) from its rotaxane, avoiding structural changes or additives. By introducing cucurbit[7]uril (CB7), the system's energy increases, causing CB6 unit release due to portal–portal electrostatic repulsion.

CURRENT STATE OF KNOWLEDGE

1 Rotaxanes

The term rotaxane is derived from the Latin words *rota* for wheel and *axis* for axle. These molecular assemblies consist of at least one macrocycle threaded onto one or more linear components. The linear component can be visualized as a sort of molecular dumbbell carrying bulky structural motifs at its ends. Both rotaxane components are mechanically interlocked as the sterically bulky groups at the ends of linear component are typically larger than the inner diameter of the cyclic compound, and therefore this complex cannot undergo dissociation. In other words, even though the axis and the macrocycle are not connected by covalent bonds, their arrangement ensures mechanical connection. A structurally similar system in which the macrocyclic molecule can slip off the axis is called pseudorotaxane.[19,20] The borderline between rotaxanes and pseudorotaxanes will be discussed below.

1.1 Synthesis of rotaxanes

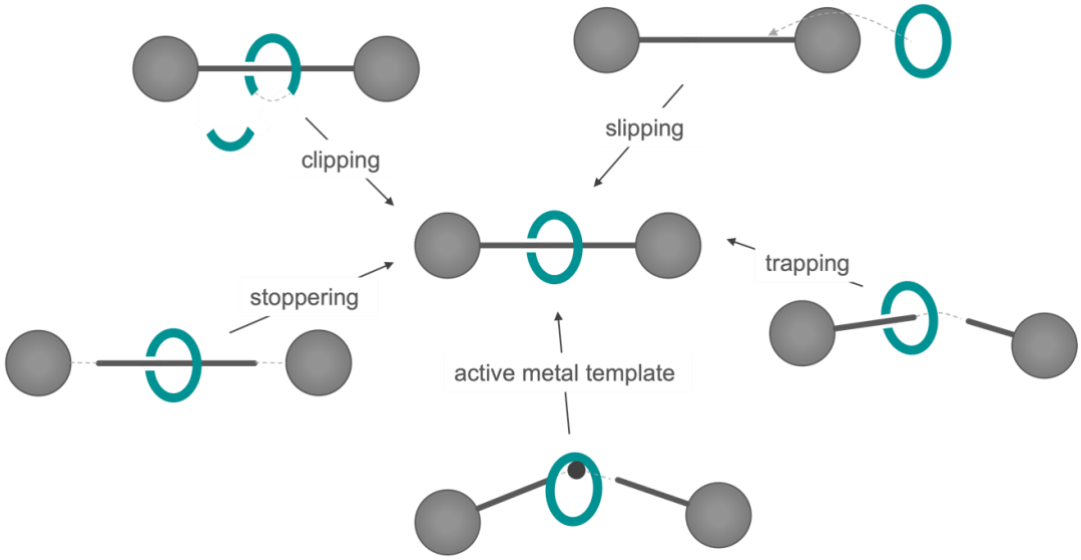

Figure 1 The most common methods for rotaxane synthesis.

Rotaxanes can be synthesized using several methods as Figure 1 illustrates. The most commonly used approaches involve the formation of a covalent bond belonging to one component of the mechanically interlocked structure in the presence of a fully preformed second component. The ring closure of an acyclic precursor of a macrocyclic compound in the presence of a molecular thread is referred to as 'clipping'.[21–23] Another synthetic strategy, the 'stoppering',[24,25] involves the formation of the dumbbell itself by attaching bulky terminal groups

to the ends of the acyclic component of the preformed pseudorotaxane. The 'trapping' method is very similar, but in this case, one half of the thread initially binds the macrocycle (forming a semirotaxane) and then covalently joins with the other half of the thread to form a rotaxane.[26] This method is often used to prepare asymmetric rotaxanes. In the case of the 'active metal template' method, the metal plays a dual role. The first is template binding, where ligands are brought into proximity within the coordination sphere of the metal atom, and the second is catalysis of the formation of a covalent bond between the reactants, which again leads to the formation of a rotaxane structure.[27–29] All four of these approaches require bond formation to be irreversible. A different strategy is used in the 'slipping' method.[30–32] Simply, it involves threading a ring onto a complete linear component that already contains terminal stopper groups in its structure. This method requires a precisely tuned size of the macrocycle and end groups so that the activation energy required for threading the macrocycle over the stoppers can be overcome under certain conditions, such as increased temperature. The resulting product must be kinetically stable upon cooling. This approach is therefore thermodynamically controlled as no new covalent bonds are formed, and it only depends on whether the resulting pseudorotaxane is more stable under threading conditions than its components. A variation of this approach is the use of a macrocyclic molecule with a sufficiently large diameter so that, even under normal conditions, the macrocycle can thread onto the axle. The subsequent chemical reaction that reduces the effective diameter of the ring leads to the transformation of the pseudorotaxane intermediate into a rotaxane (the 'shrinking' method).[33,34] Conversely, a pseudorotaxane containing small stoppers that do not significantly hinder the movement of the macrocycle, can be converted into a rotaxane by enlarging these end groups (the 'swelling' method).[35,36]

Since my doctoral thesis focuses on the synthesis of rotaxanes using the slipping approach, this method will receive particular emphasis.

Slipping method

In 1993, Stoddart first reported the synthesis of a rotaxane consisting of bis-paraphenylene[34]crown-10 macrocycle and a series of 4,4'-bipyridinium linear components using the slipping method.[30] In this strategy, the macrocycle along with the linear component is heated to such a temperature that the energy barrier $\Delta G^{\ddagger}_{on}$ required for the macrocycle to slip over the stoppers of molecular axle is overcome. The resulting rotaxane structure is then kinetically trapped by cooling the equilibrium mixture to room temperature, preventing the system from overcoming the $\Delta G^{\ddagger}_{off}$ barrier. In other words, this energy barrier prevents the dethreading of the macrocycle from the resulting interlocked structure (Figure 2).[37] Unlike previous methods, all the covalent bonds forming the

molecular components of the rotaxane are already created in previous synthetic steps.[38]

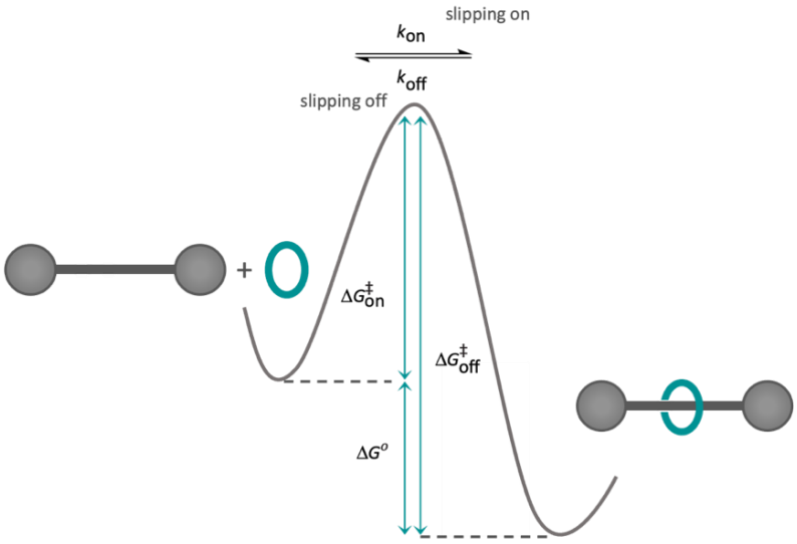

Figure 2 Schematic representation of the energy diagram in the formation of rotaxanes using slipping method.

Eric Masson's publication[39] was an inspiration to us in the design and synthesis of our rotaxane structures. His work explored how varying N^1-substituents affect CB6 slippage along N^1,N^6-disubstituted hexane-1,6-diammonium salts **24a–d** (Figure 3), with the N^6-substituent serving as s stopper. Thermal activation enabled the formation of stable rotaxanes, driven by CB6's strong affinity for diammonium salts,[40] with the first-order kinetics favoring interlocked structures, with negligible reverse reaction.

Slippage rates varied significantly with small steric differences. For example, at 373 K, half-lives ranged from seconds (cyclopropyl) to hours (isopropyl), while trifluoroethyl caused high barriers due to electrostatic repulsions. Negative entropy changes arose from constrained motion of CB6 distortion. Computational studies revealed a multistep mechanism involving deprotonation, neutral amine passage, and reprotonation, emphasizing the sensitivity of slippage to steric and electronic factors.

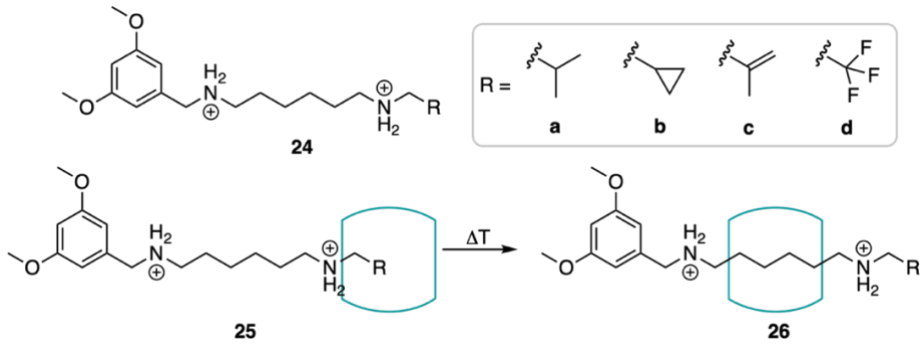

Figure 3 A series of rotaxane structures studied by Masson.

1.2 Rotaxanes versus pseudorotaxanes

Pseudorotaxanes can be relatively easily distinguished from rotaxanes by whether the bulky groups at the ends of linear component can prevent the dethreading of the cyclic component or not. When the stoppers are bulky enough to prevent dethreading of the cyclic component, we usually call it rotaxane. If not, the system is referred to as a pseudorotaxane.[41] It should be noted that the dethreading through the bulky substituents can be accelerated by higher temperatures, making the term (pseudo)rotaxane a function of temperature. Therefore, it is not surprising that there are such boundary structures where it is not always obvious at first glance whether it is one situation or the other. So where do we draw the line between the rotaxanes and pseudorotaxanes? In other words, when does such a complex cease to be a pseudorotaxane and become a rotaxane?

Researchers in 1998 explored the stability of [2]pseudorotaxanes and their conversion into rotaxanes using thermal energy and structural modifications.[42] They found that the stability of these structures depended heavily on solvent polarity; nonpolar solvents favored the formation of kinetically stable rotaxanes, while polar solvents caused dissociation, highlighting the dual nature of pseudorotaxanes as intermediated between interlocked and isolated entities (Figure 4).

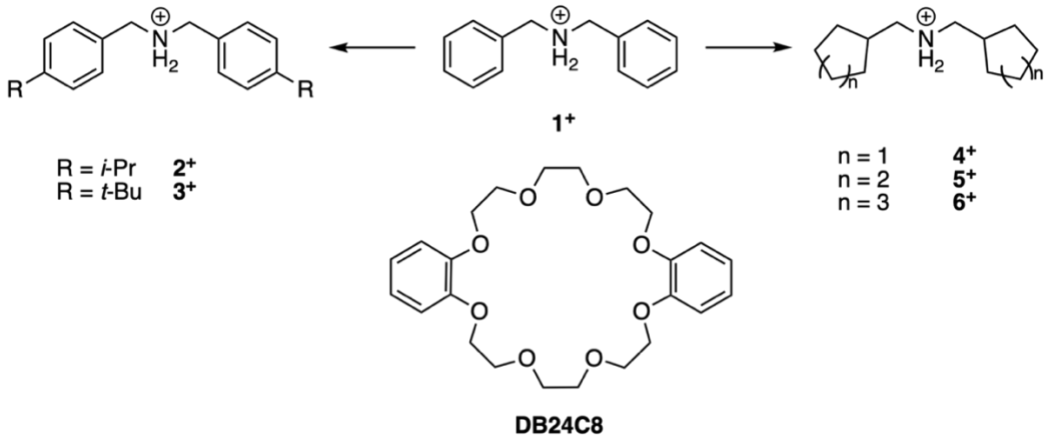

Figure 4 Structural modification of **1**$^{+}$ leading to suitable axles for the synthesis of rotaxane structures using slipping method.

In 2001, further studies examined how structural factors influence the deslipping kinetics of rotaxanes.[43] It was observed that minor changes in stopper geometry, ligand flexibility, and hydrogen bonding significantly impacted the stability of these complexes. Spherical substituents were more effective at hindering deslipping than planar ones, disproving earlier hypothesis that rotaxane stability relies solely on mechanical interlocking.

The concept of metastable rotaxanes was also developed, describing structures with stability that depends on environmental conditions such as temperature and solvent polarity. These metastable systems have potential applications in areas like drug delivery[44–47] and molecular memory.[48,49] For example, a doubly threaded [3]rotaxane was designed with tunable stability, achieving half-lives ranging from minutes to several months.[50]

In 2017, a [2]rotaxane with ferrocene stoppers and an azobenzene central motif that exhibited light-induced dethreading was described.[51] The addition of CB7 stabilized the structure *via* strong noncovalent interactions, expanding the range of possible rotaxane designs beyond traditional covalent stoppers (Figure 5).

Finally, multitopic host molecules were developed in our group by combining biphenylene(bis)imidazolium with adamantly motifs, which formed diverse pseudorotaxane and rotaxane assemblies with CB7 and β-CD.[52] These advanced supramolecular systems showcase the versatility of host–guest chemistry in creating complex and functional materials.

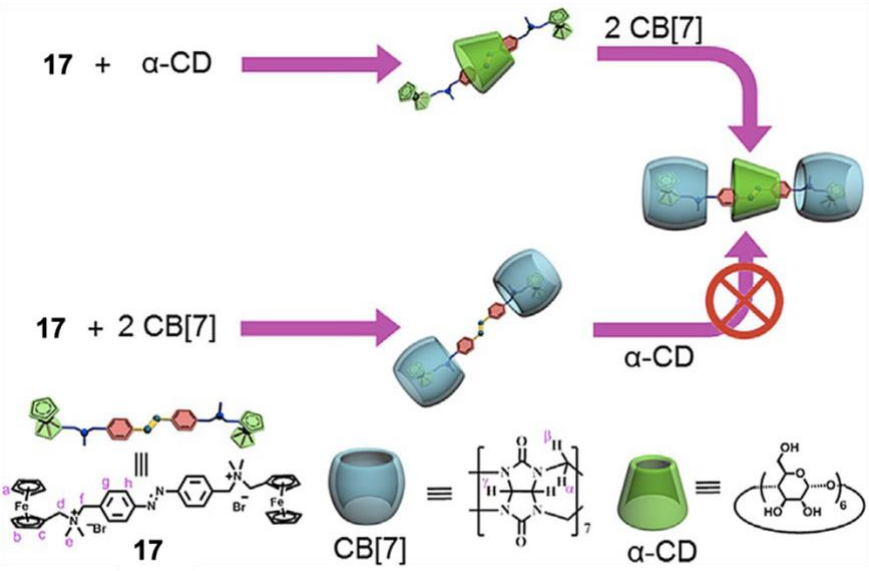

Figure 5 Construction of the pseudorotaxane and rotaxane.[51]

1.3 Responsive molecular systems

Responsive rotaxane systems are valued for their unique interlocked structures and dynamic properties, enabling controlled molecular movement. Stoddart's pioneering work[53] established the concept of molecular shuttles and switches, where macrocycles move between distinct recognition sites in response to external stimuli like pH, redox changes, light, or ion binding. These mechanisms have led to innovations like rotaxane-based molecular machines, catalysis, and drug delivery systems. For instance, pH-responsive rotaxanes regulate catalytic

site access by shifting macrocycles between recignition sites based on protonation states.[54] This concept extends to complex systems like molecular nanoelevator, developed by Stoddart's group, where acid-base stimuli control vertical movement (Figure 6).[55]

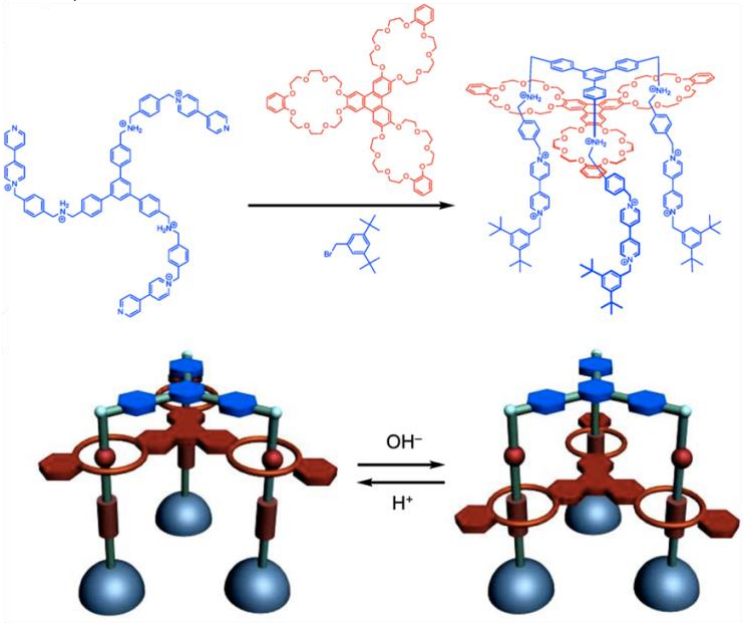

Figure 6 Acid/base controlled nanoelevator.[55]

Light-driven rotaxanes[56,57] exhibit position switching for applications in information storage and catalysis (example in Figure 7). Such systems promise advancements in nanotechnology, medicine, and functional materials. Enzymatic activation has also been explored in rotaxane-based systems. A biocompatible rotaxane system designed for the controlled release of an anticancers drug inside cancer cells is a prime example (Figure 8).[58]

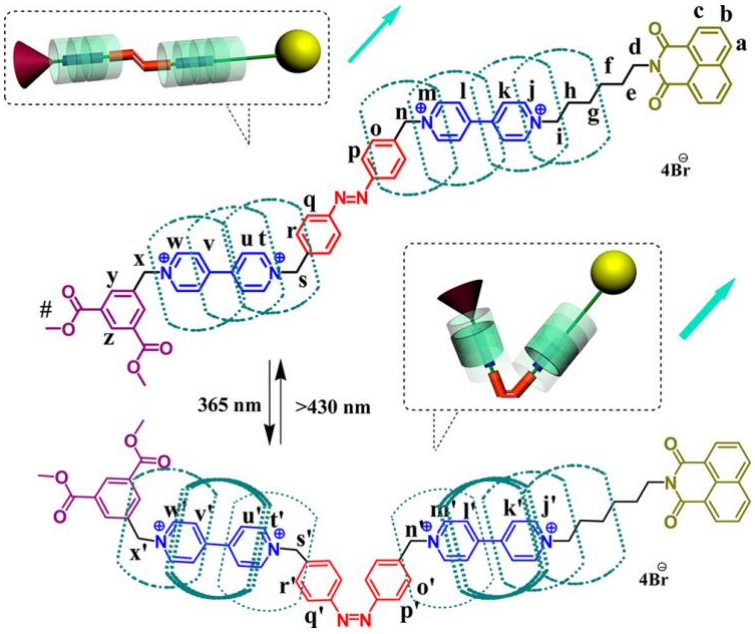

Figure 7 Light-controllable [3]rotaxane.[56]

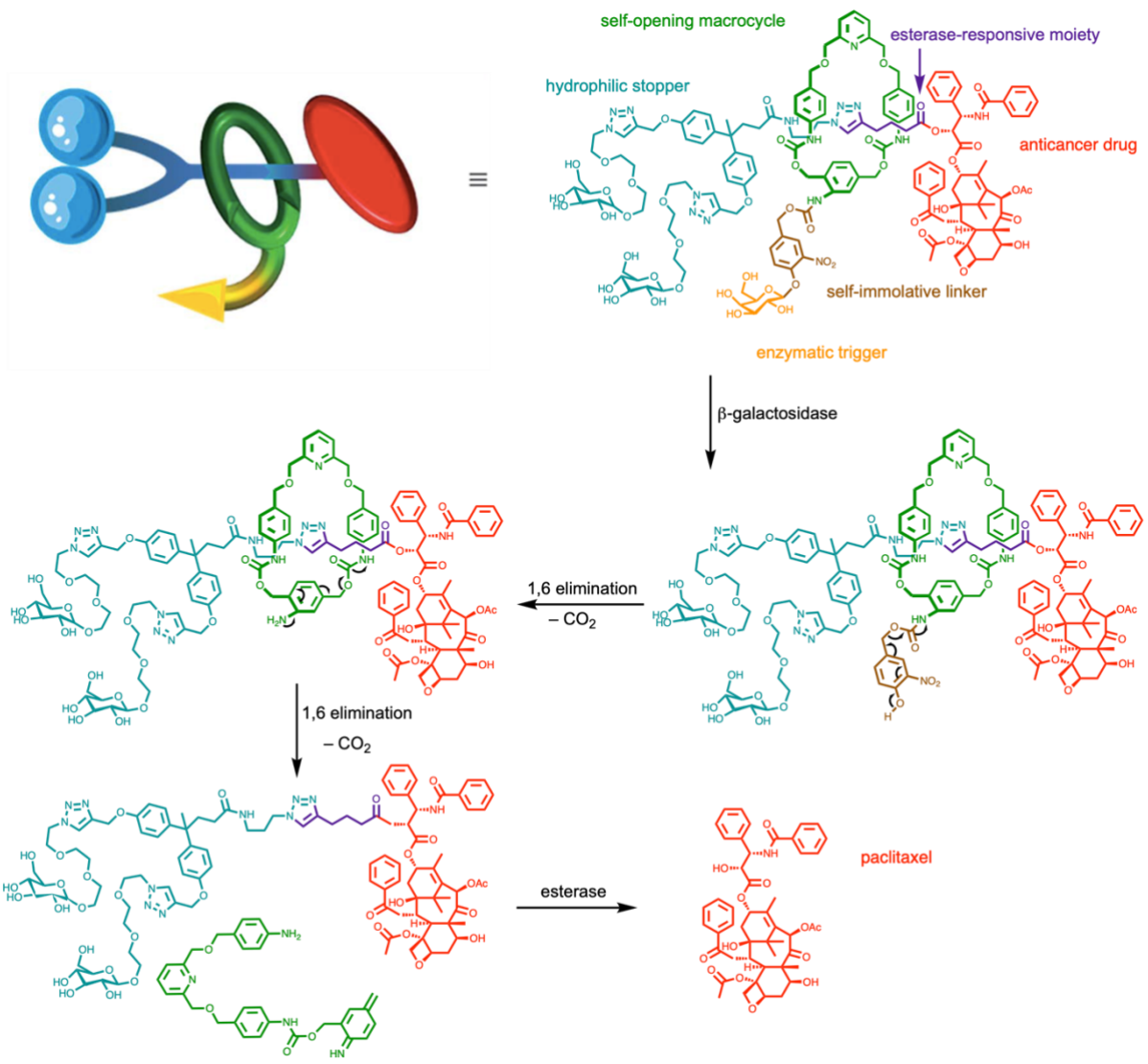

Figure 8 Structure of a biocompatible [2]rotaxane and mechanism of paclitaxel release within cancer cells (modified according to[58]).

RESULTS AND DISCUSSION

Introduction

The research carried out by our supramolecular chemistry group focuses on two complementary areas. First of them is aimed to the design and synthesis of model compounds containing new binding motifs based on bulky cage-like hydrocarbons, e.g., adamantane, diamantane, bicyclo[1.1.1]pentane or spiro[3.3]heptane as well as the study of their supramolecular behaviour. The purpose of the second area of our interest is to rationally design and synthesize new supramolecular ligands with multiple binding sites, so-called multitopic ligands, and subsequently investigate their supramolecular behaviour towards macrocyclic host molecules based on cyclodextrins and cucurbit[*n*]urils. The knowledge obtained by supramolecular data analysis of the prepared complexes subsequently provide the essential understanding necessary for the design of more complex, so-called advanced functional host–guest systems. These systems have a strong potential to be used in the field of chemical molecular sensors, probes, catalysts, or as drug delivery systems.

The ligands in such systems should have the ability to bind more than one macrocycle. This is conditioned by the presence of various binding sites that exhibit different affinities towards individual macrocyclic compounds. To achieve such a task, the values of association constants (*K*) of individual binding sites should be as high as possible and simultaneously significantly different from each other. Thus, each binding site would exhibit specific binding for particular host molecule. Based on carefully selected differences between the *K* values, it should be possible to prepare a stable system that can be potentially rearranged by, for example, chemical or thermal stimulus.

Since we have been studying mutual interactions between macrocycles bound simultaneously to one molecular thread for a long time,[52,59–62] at the beginning of my research we were particularly interested in the structures of linear molecular guests that carry bulky terminal groups serving as stoppers for the macrocycle bound on the central part of the ligand and also as another binding sites for other macrocycles. The idea was that these systems would offer us a detailed study of the mutual interactions between macrocycle bound at the terminal site and the macrocycle that cannot leave the system. This, in turn, would help us to understand the role of portal–portal interactions between host molecules and competition/compensation effect in overall complex stabilisation.

To the best of our knowledge, rotaxanes are best suited for these purposes, since by definition they contain a linear and a cyclic molecule that is kinetically interlocked in the system by bulky terminal motifs at the ends of the linear

component. In addition, we can appropriately modify the terminal bulky moieties to act as high affinity binding sites for CB*n*s and CDs.

In the following chapters, I will tell the story of three generations of rotaxane systems that accompanied me during my doctoral study (Figure 9).

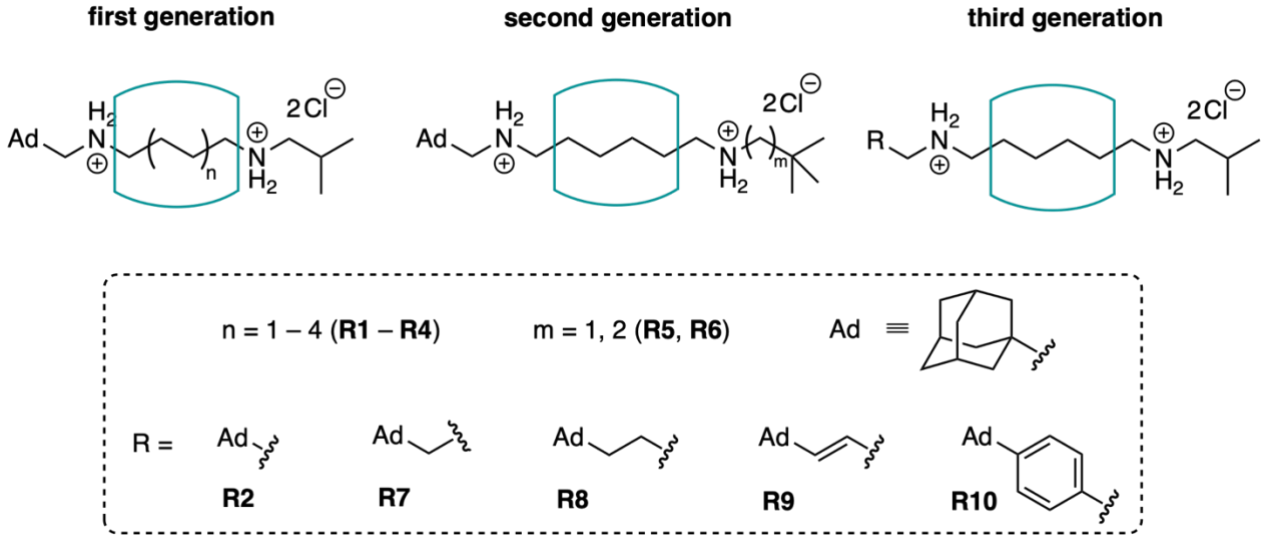

Figure 9 The structures of three generations of rotaxanes, whose development is described in this work.

2 First-generation rotaxanes

The first generation of our guests consists of an isobutyl stopper (IB) which enables threading of CB6 at high temperature, protonated α,ω-alkyldiammonium linker of variable length representing the binding site for CB6 and terminal adamantane-based high-affinity binding site for the second macrocycle (CB7, β-CD). The initial idea for this design was that longer linkers would allow movement of the rotaxane macrocycle, potentially enabling the quantification of repulsions/attractions between the macrocycles bound at the rotaxane site and the terminal positions.

Synthesis of ligands L1–L4

A four-step synthetic pathway leading to the N^1-N^6-disubstituted α,ω-alkyldiammonium salts, desired ligands **L1**–**L4** (the axles of the intended rotaxanes), is depicted in Scheme 1. Their structures and purity were confirmed by ^{1}H, ^{13}C and 2D NMR spectra and ESI-MS analysis.

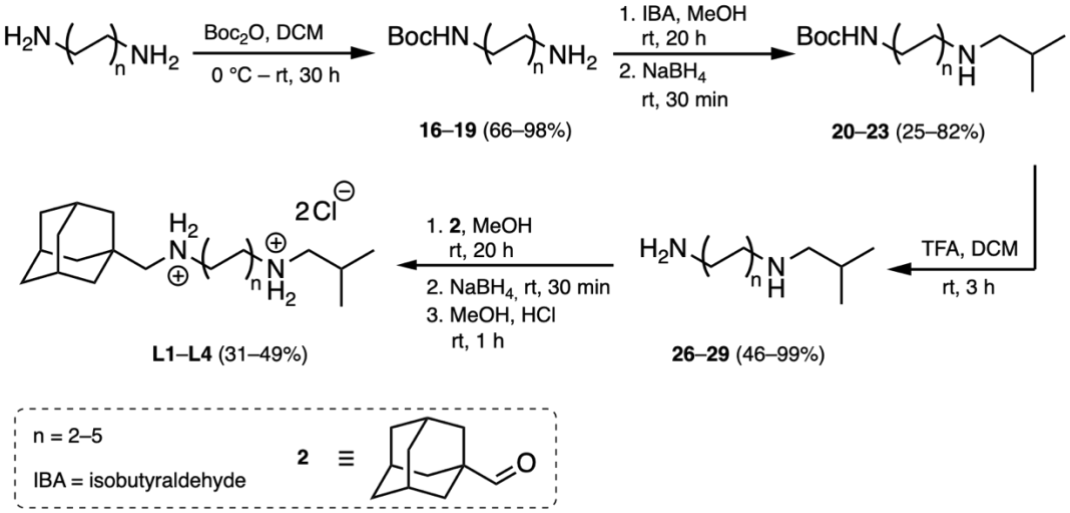

Scheme 1 Synthetic pathway leading to the first-generation ligands **L1**–**L4**.

Formation of rotaxanes R1–R4

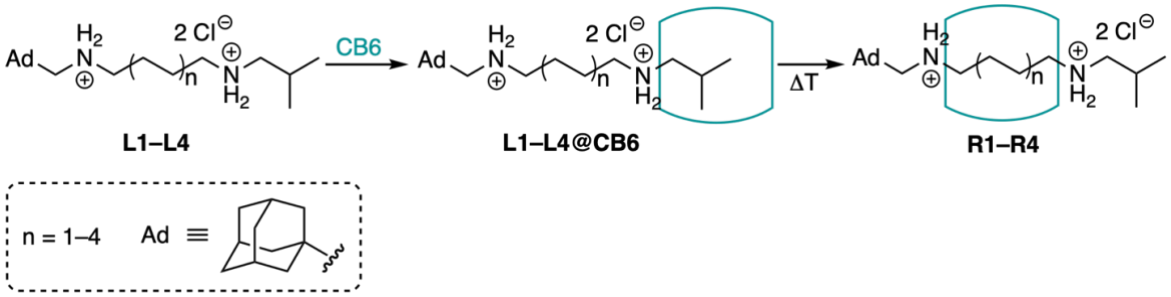

Scheme 2 Formation of first-generation rotaxanes **R1**–**R4**.

The first step after mixing equimolar amounts of ligands **L1**–**L4** with CB6 in a 50 mM NaCl solution is the formation of **L**@CB6^{IB} complexes (Scheme 2). The formation of such inclusion complex was easily confirmed by ^{1}H NMR analysis, where signals of H-atoms belonging to the IB terminal moiety shift towards a higher field. This is typical for H-atoms located within the complex inside the CB*n*s (Figure 10).

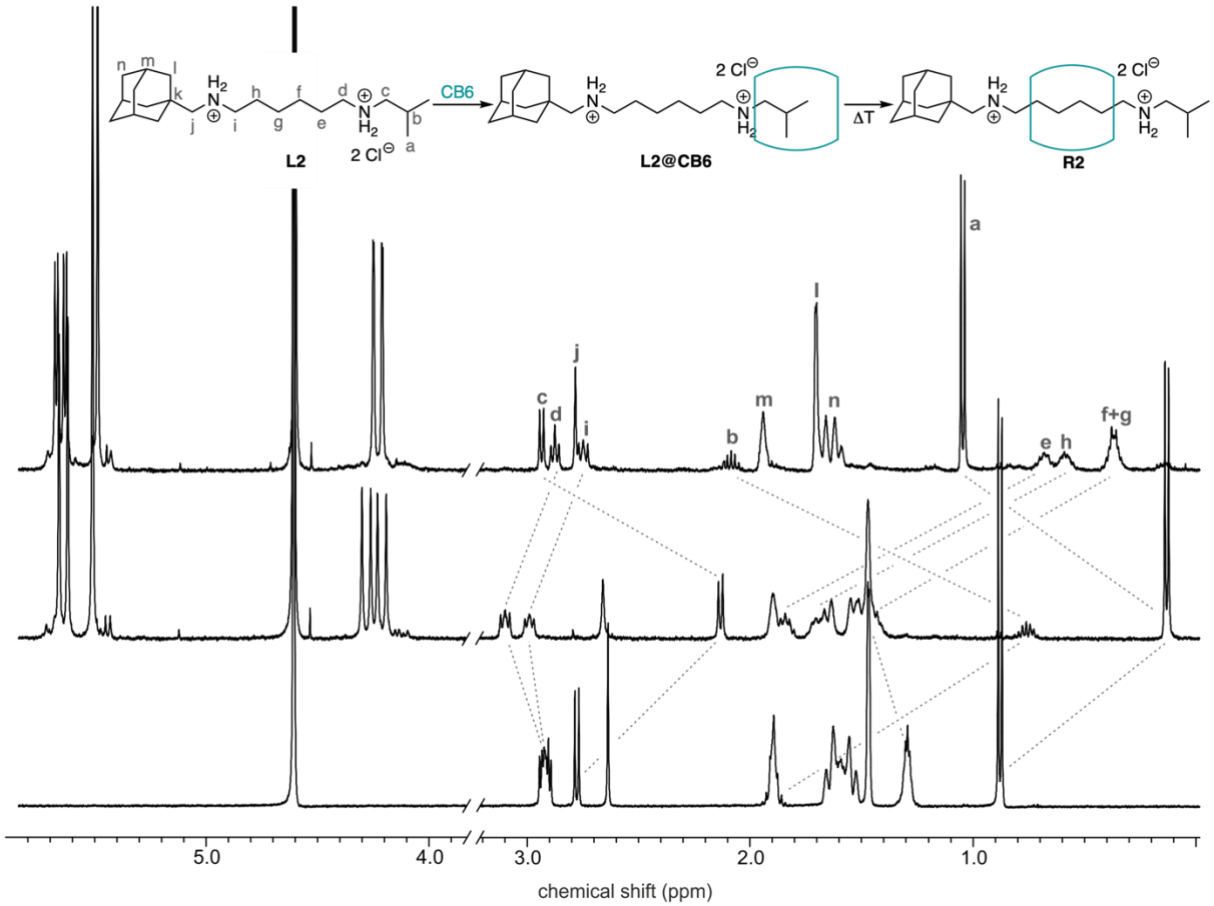

Figure 10 ^{1}H NMR spectra of individual steps of rotaxane **R2** formation (bottom line: **L2**; middle line: **L2**@CB6^{IB}; upper line: **R2**).

After thermal treatment (MW reactor, 300 W, 1.4 MPa) of these complexes in aqueous medium at 393 K for two hours, CB6 slipped through the terminal isobutyl stopper to the central binding site. After cooling the system to room temperature, the CB6 was kinetically trapped by the stoppers to form rotaxanes, as illustrated in Scheme 2 (confirmation of rotaxanes stability is commented later). The formation of rotaxane can also be easily confirmed by ^{1}H NMR. The signals corresponding to the H-atoms of the IB terminal moiety *a*, *b*, *c* have significantly shifted downfield, indicating their location near the carbonyl portals of CB6. On the contrary, the H-atoms from the central alkyl linker *d*–*i* are significantly shielded, as they are now located inside the macrocycle. However, this ideal situation occurred only in the case of rotaxane **R2** as the equilibrium between CB6, diammonium salt and complex **L2**@CB6 (involving two

transformations: CB6+**L2** to **L2**@CB6^{IB} and then this complex to **R2**) is significantly shifted towards the interlocked structure and the concentrations of free components and **L2**@CB6^{IB} are negligible. This concerts with the fact that affinity of CB6 towards the hexamethylenediammonium central linker (HMDA) is much greater than towards terminal primary alkylammonium cation. Association constant for hexane-1,6-diammonium@CB6 complex is 7.9×10^{9} M^{-1} (determined in 2.5 mM NaCl using ITC).

On the other hand, the desired rotaxanes **R1**, **R3** and **R4** could not be successfully isolated because, during their formation, the equilibrium concentration of the complexes with CB6 positioned on the central parts was insufficient. The data in Table 1 clearly show a relationship between binding strength, CB6 selectivity towards individual motifs, and rotaxane formation.

These results indicate that high binding affinity and a optimal molecular guest fit within the CB6 cavity are crucial for efficient rotaxane formation (comparison of dimensions of CB6 and variable α,ω-alkyldiammonium ions see in Figure 11).

Table 1 Association constants *K*, selectivity of CB6 towards binding motifs and NMR conversions of **L**@CB6^{IB} complexes to rotaxanes.

K (M^{-1})[a]	selectivity of CB6	NMR conversion
IB@CB6, 5.33×10^{5}		
HMDA@CB6, 2.9×10^{8}	HMDA/IB 544	91%
BDA@CB6, 2.0×10^{7}	BDA/IB 37.5	85%
ODA@CB6, 1.1×10^{6}	ODA/IB 2.06	14%
DDA@CB6, 1.7×10^{4}	DDA/IB 0.03	0%

[a]measured using ITC in 50 mM NaCl

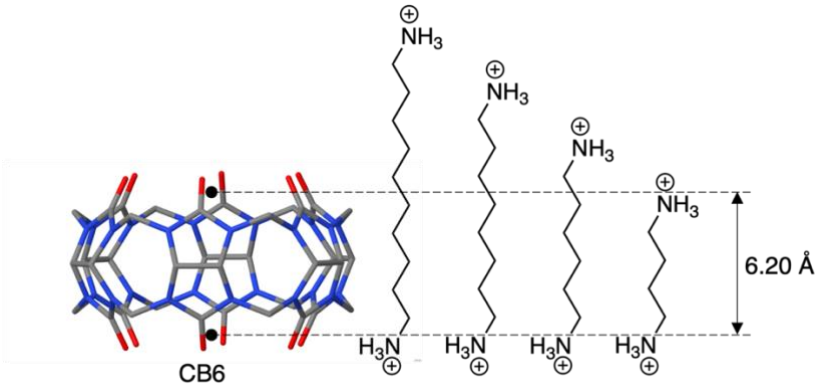

Figure 11 Comparison of dimensions of CB6 and variable α,ω-alkyldiammonium ions.

NMR supramolecular studies on R2 with β-CD and CBs

Considering that CDs generally enable the formation of host–guest complexes with hydrophobic part of the ligands and are primarily stabilised by van der Waals interactions and hydrophobic effect, we assumed that β-CD would bind solely to the Ad binding site, which, due to its shape and size, fits almost perfectly into the β-CD cavity. These assumptions were confirmed by ^{1}H NMR titration.

In case of complexation with CB6, according to ^{1}H NMR, there is no binding of the macrocycle to the preferred IB terminal. There is simply not enough space for complex formation due to the strong repulsion between the carbonyl portals of the additional CB6 and the CB6 that was already interlocked within the system.

On the other hand, complexation of rotaxane **R2** with CB7 revealed very surprising behaviour. We expected binding of CB7 to the Ad binding site, which was confirmed using ^{1}H NMR (Figure 12). However, the signals from the central part *d*–*i* were deshielded, while the signals from the IB moiety *a* and *c* were simultaneously shielded, suggesting a shift of CB6 from the central to the terminal IB site. This observation suggests that the repulsion between the CB7 and CB6 is sufficient to overcome the energy barrier (121.3 kJ·mol^{-1}, as reported by Masson) for dethreading the CB6 from the rotaxane axle at 303 K. It is worth reiterating that the CB6 slipping on takes 2 hours at 393 K to form the rotaxane **R2**. These preliminary results were extensively elaborated on the series of the third-generation ligands and will be discussed later.

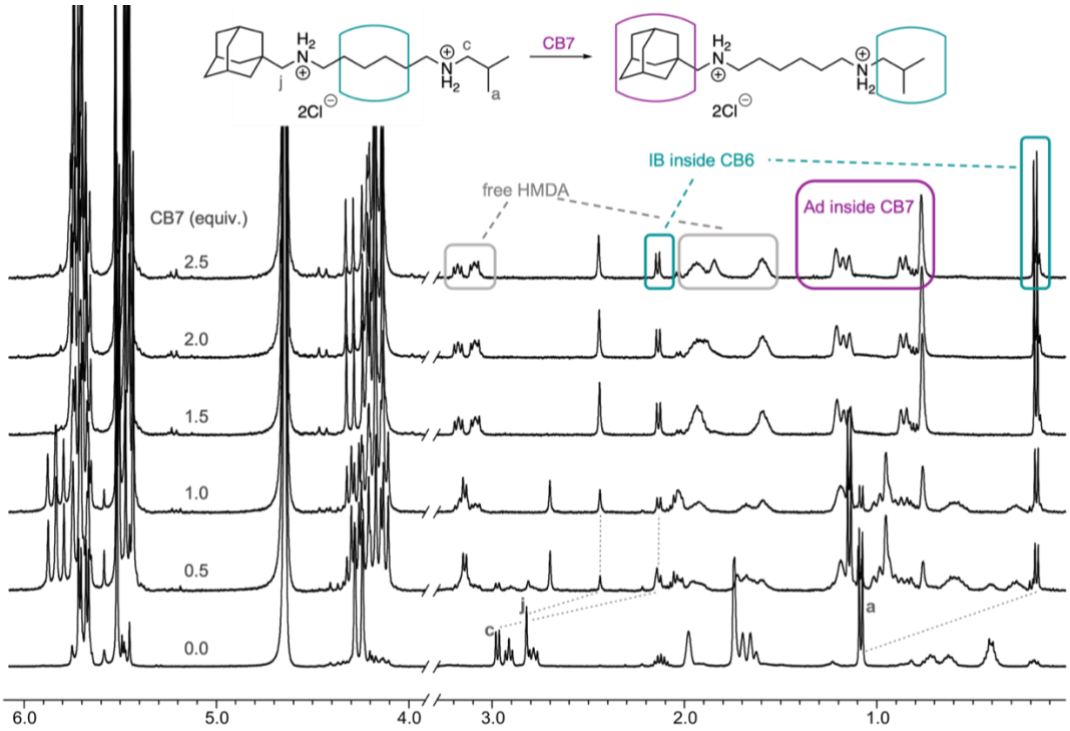

Figure 12 Stacking plot of ^{1}H NMR spectra recorded within the titration of rotaxane **R2** with CB7.

Due to the **R2** dethreading upon complexation with CB7, we decided to prepare a second-generation ligands/rotaxanes before proposing other experiments for this rotaxane. In this new generation, the stopper will be somewhat bulkier than the IB motif. Hypothetically, this modification should prevent the dethreading of CB6 from its rotaxane site after complexation with CB7.

3 Second-generation rotaxanes

For the reasons stated at the end of the last chapter, we decided to keep the length of the alkyl centre chain for six carbon atoms (like **L2** has) and modify the the terminal binding site, which enables temperature-dependent threading of CB6 onto the axle. The modification involved enlarging this group, and for this purpose, a *tert*-butyl motif (TBU) was selected.

Synthesis of ligands L5 and L6

Synthetic strategy leading to the second-generation ligands **L5** and **L6** is depicted in Scheme 3. The structures of ligands **L5** and **L6** were confirmed by 1D, 2D NMR and ESI-MS analysis.

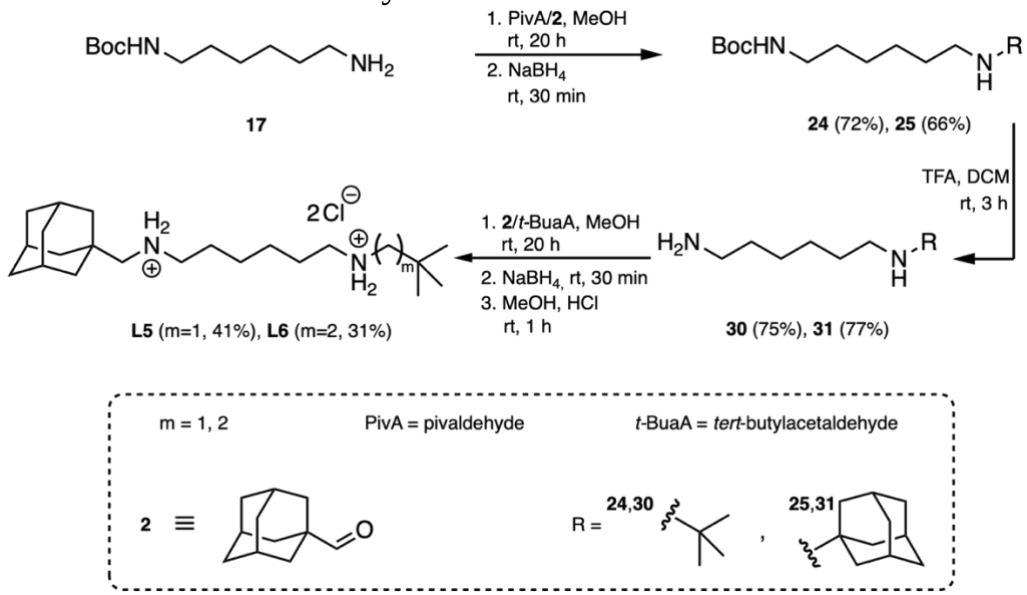

Scheme 3 Synthetic pathway leading to the second-generation ligands **L5** and **L6**.

Formation of rotaxanes R5 and R6

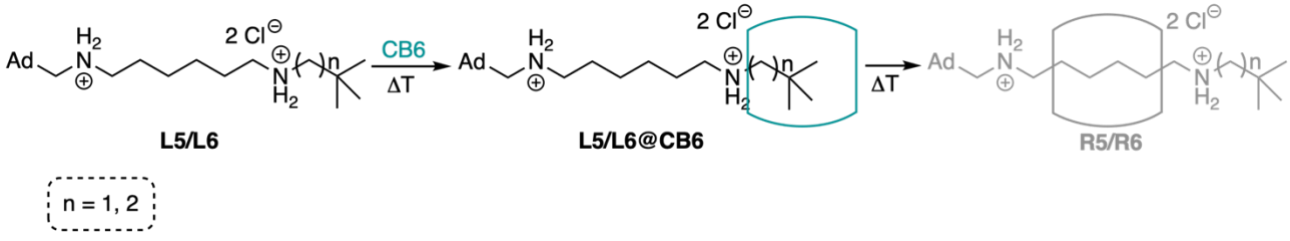

Scheme 4 Formation of second-generation rotaxanes **R5** and **R6**.

The preparation of complexes **L5**/**L6**@CB6 was investigated under various conditions. In case of **L5**@CB6, heating the mixture of ligand with 1.5 equiv. of CB6 to 333 K for 40 hours was required for complex formation (Scheme 4), as ambient temperature was insufficient. The complex formation was confirmed by changes in NMR spectra, indicating shielding of signals from TBU terminal motif by the H-atoms from CB6 macrocycle. However, attempts to synthesize the rotaxane **R5** under the same conditions as **R2** were unsuccessful, even with extended reaction times and higher temperatures (Figure 13).

Similarly, the **L6**@CB6 complex required gradual heating, with the maximum complex formation (40%) achieved at 368 K after 19 days. Despite attempts to synthesize the **R6** using microwave reactor, no successful formation was observed. In both cases, the desired rotaxanes were not obtained, highlighting challenges in overcoming the energy barrier for rotaxane formation.

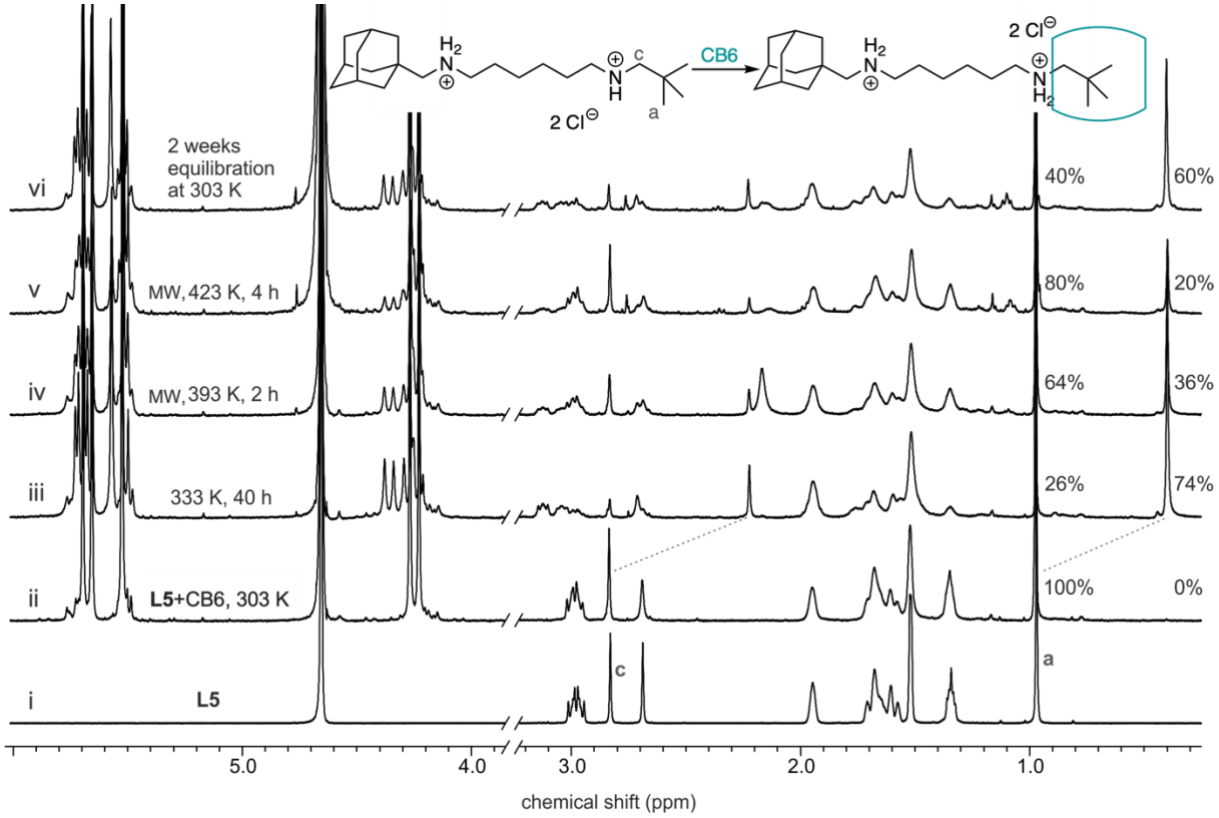

Figure 13 ^{1}H NMR spectra of **L5** and CB6 mixtures (1:1 in 50 mM NaCl solution in D_2O); MW = microwave.

Since we were unable to prepare rotaxanes **R5** and **R6** with bulkier terminal motif than IB, and to prevent the dethreading the CB6 upon binding with CB7, we opted to alter the other end of the molecular probe, which will be described in the following chapter.

4 Third-generation rotaxanes

In designing the third-generation structures, we modified the opposite side of the ligand compared to the second generation. The high-affinity Ad binding site was retained, with the key parameters of the newly designed molecular probes being the length of the linker between Ad and the positively charged nitrogen, and its rigidity to a certain extent. Thus, we proposed five different adamantane-derived ammonium terminal motifs with methylene to phenylenemethyl spacer.

4.1 Synthesis of ligands and rotaxanes

Synthesis of ligands L2, L7–L10

Ligands of the third-generation **L2**, **L7**–**L10** were also synthesised *via* sequence of Boc protection/deprotection, Schiff base formation, and reduction from hexane-1,6-diamine and aldehyde precursors of the terminal moieties, as Scheme 5 shows. For simplification, the reaction scheme starts with compound **27**, which had already been prepared to synthesise the ligands of the first generation. Ligand **L2** naturaly belongs also to this third-generation set. The structure of ligands **L7**–**L10** was confirmed by 1D, 2D NMR and ESI-MS analysis.

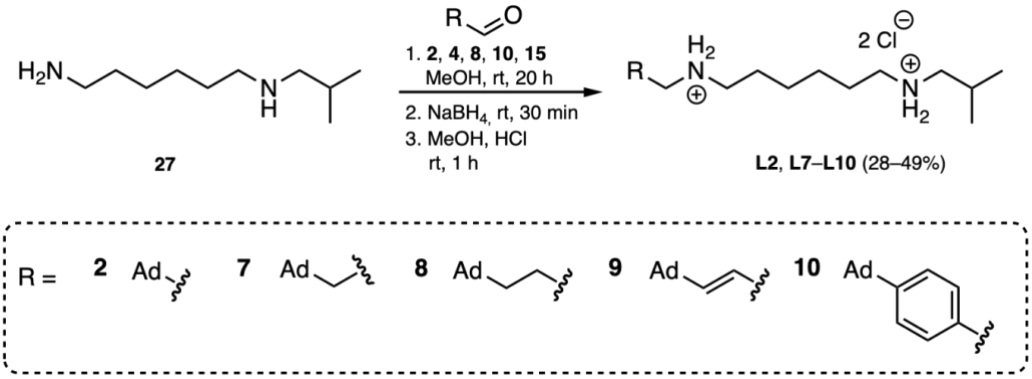

Scheme 5 Synthetic pathway leading to the third-generation ligands **L2**, **L7**–**L10**.

Formation of rotaxanes R2, R7–R10

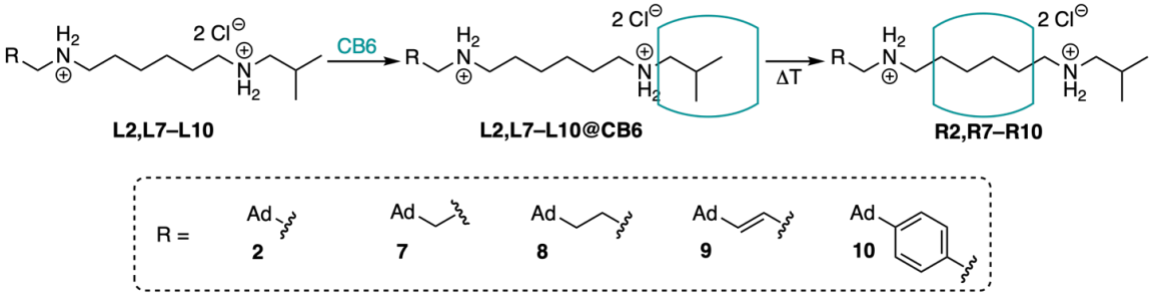

Scheme 6 Formation of third-generation rotaxanes **R2**, **R7**–**R10**.

Since the third-generation ligands contain the IB terminal moiety and the central hexane-1,6-diammonium linker as the key components for threading of CB6, the formation of third-generation rotaxanes was analogous to the formation of rotaxane **R2**, as Scheme 6 shows.

Although the synthesis of these rotaxanes was successful, approximately 9% of **L**@CB6^{IB} complexes still remain in the crude products. For the purpose of further supramolecular experiments, purification of rotaxanes was performed. For this purpose, we developed suitable method using column chromatography with a highly polar mobile phase (H_2O/MeCN/HCOOH, 5/2/1, v/v/v). The structure and purity of rotaxanes **R2**, **R7**–**R10** was confirmed by 1D, 2D NMR and ESI-MS analysis. We also succeeded in growing single crystals of **R2** and **R7**–**R9** and X-ray diffraction analysis confirmed the positioning of the CB6 unit at the HMDA binding site (see Figure 14).

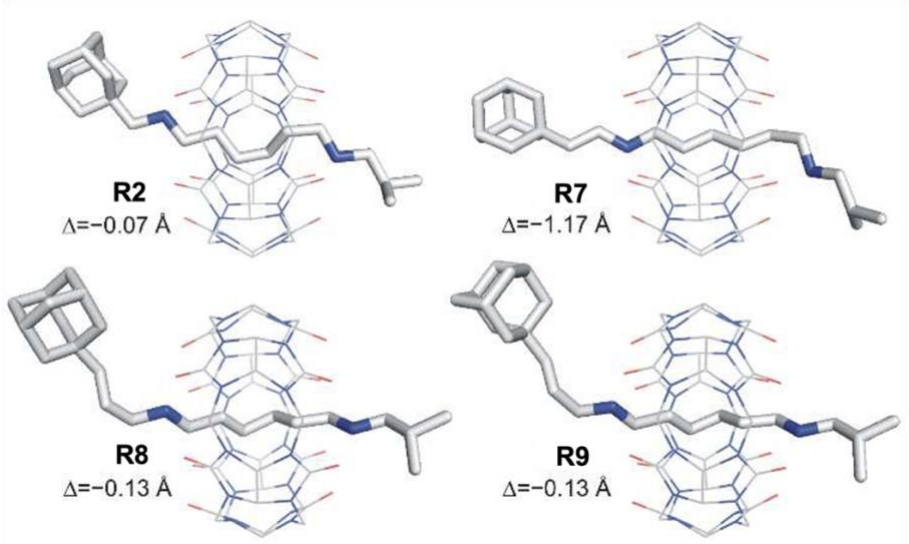

Figure 14 X-ray structures of of **R2** and **R7**–**R9**. Minor disordered atoms, solvents, anions, and H-atoms are omitted for clarity. Δ = distance between centres of HMDA site and CB6 unit.

4.2 Testing the stability of rotaxanes

To verify the long-term stability of rotaxane **R2** in water, we performed several competitive experiments with HMDA and spermine (SP). Mixing **R2** with equimolar or double amount of HMDA ($K = 2.9\times10^8\ M^{-1}$, ITC in 50 mM NaCl[40]) in D_2O showed no dethreading of CB6 even after 5 months. Similarly, no dethreading was observed with SP ($K_{SP@CB6} = 3.3\times10^9\ M^{-1}$, ITC in 50 mM NaCl[40]) after 3 months. From this reasons, we considered the structures **R2** and **R7**–**R10** as kinetically interlocked rotaxanes at room temperature.

4.3 Supramolecular studies – NMR titrations

NMR titration experiments with ligands

β-CD binds naturally to the adamantane site of the ligands, while CB6 forms complexes with ligands **L2** and **L7**–**L10**, binding to the isobutyl ammonium site. The stoichiometry of both complexes is 1:1.

In contrast, the ligands have up to three binding sites for CB7, making the titrations more complex. Initially, CB7 bound to the high-affinity Ad site. As more CB7 was added, the shifts of signals were still observed, resulting in a 1:2 **L**@CB7^{Ad,IB} complex (Figure 15). Despite a higher affinity for the HMDA site, CB7 binds to the IB site due to repulsion between two CB7 molecules.

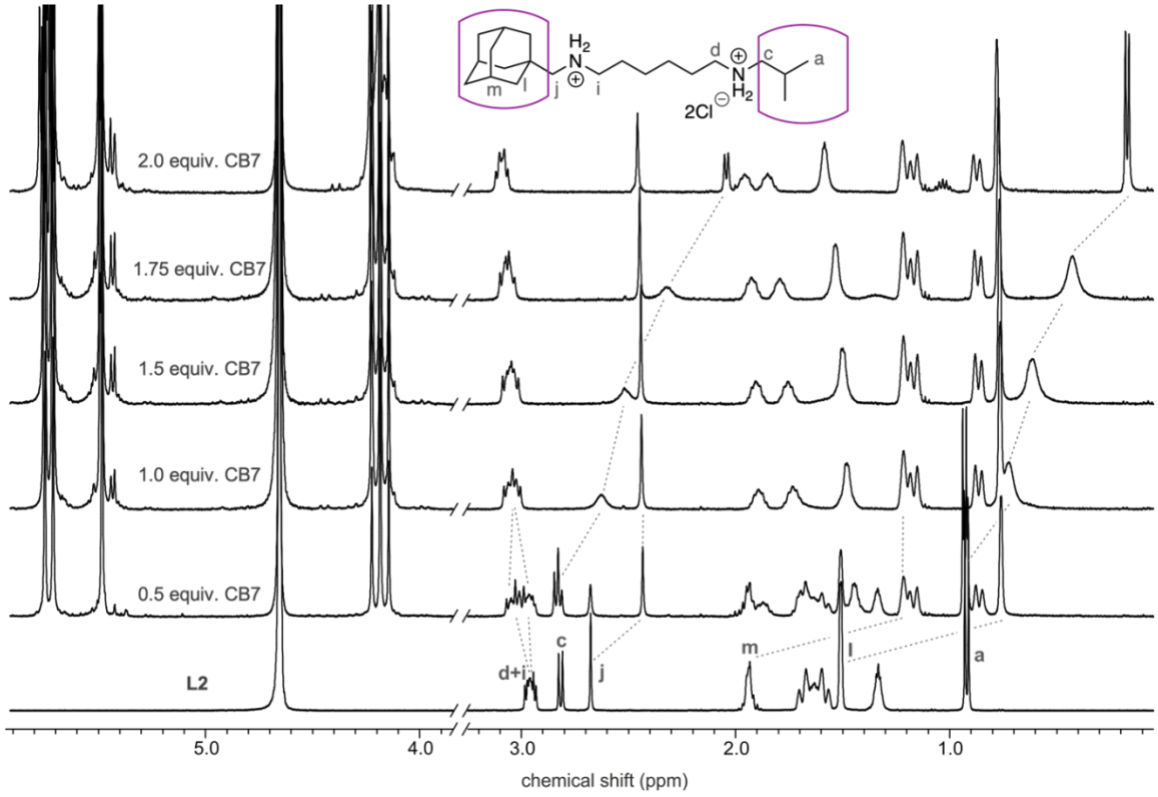

Figure 15 Stacking plot of ^{1}H NMR spectra recorded within the titration of ligand **L2** with CB7.

NMR titration experiments with rotaxanes

The results of titrations of rotaxanes **R7**–**R10** with β-CD and CB6 are similar to the results for **R2**. β-CD binds to the Ad binding site of the ligands, forming complexes with a 1:1 stoichiometry. As for CB6, there is no observable complexation due to the repulsions between the interlocked CB6 and the CB6 macrocycles potentially bound at the IB site.

The complexation of rotaxane **R2** with CB7 brought exciting results, as described earlier. And so that, due to the repulsion between the macrocycles, CB6 slipped off the rotaxane axle even at a temperature of 303 K. So we held a particular interest in the outcome after the complexation of rotaxane **R7** with CB7. Whether CB7 on Ad will trigger the release of CB6 from its rotaxane position or not. Figure 16 shows that when CB7 binds to the Ad terminal site of **R7** at 303 K, rotaxane remained intact, as no additional signal shifts were observed. This suggests that only one additional methylene group, i.e. a small extension of the linker between the Ad and a positively charged nitrogen atom, significantly decreases repulsion between the macrocycles. This means that rotaxane is considered stable even after the complexation with CB7 at room temperature. We observed similar behaviour in case of complexes **R8**–**R10** with CB7 as well. Thus, an important question arose: Does this behaviour also apply at elevated temperatures?

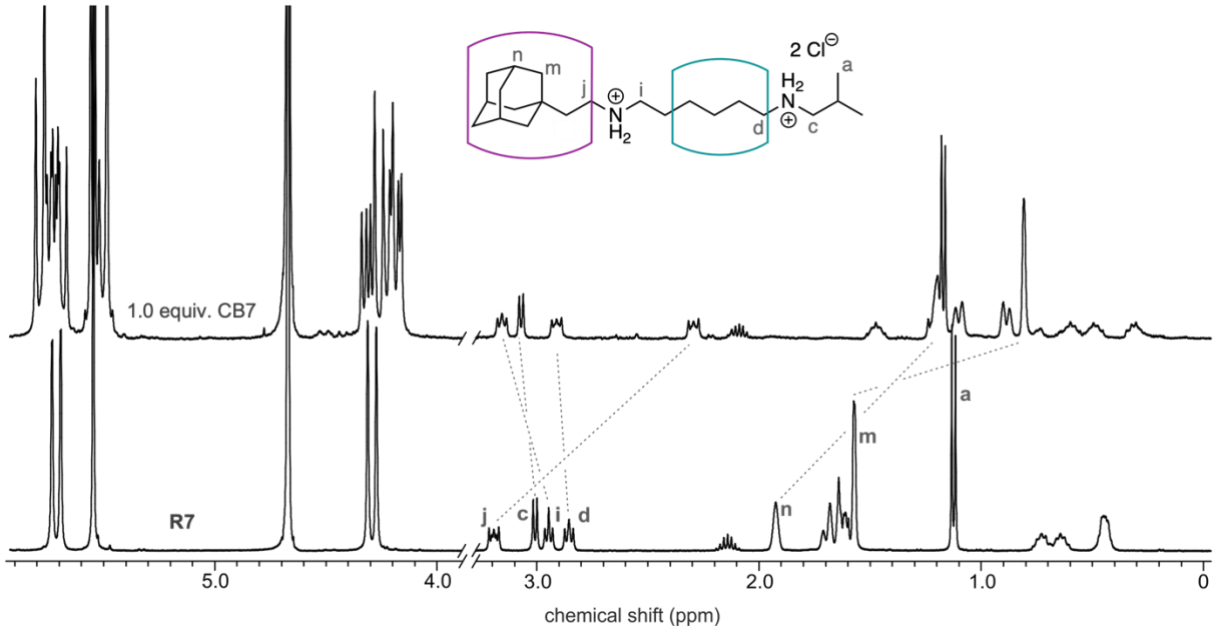

Figure 16 ^{1}H NMR (D_2O, 303 K) spectra of rotaxane **R7** (bottom) and its equimolar mixture with CB7 (top).

4.4 Supramolecular studies – kinetic experiments

Kinetics of the rotaxanes dethreading process

Initially, we performed a series of experiments for rotaxane **R2** (0.85 mM) with CB7 (1:1), starting with kinetic experiment at 303 K. The first and the last ^{1}H NMR spectra are illustrated in Figure 17 (**1**). In the initial step, CB7 binds to the Ad, resulting in an upfield shift of signals of the H-atoms at the Ad cage, and, simultaneously, H-atoms of the IB end (*a*, *c*) were slightly deshielded. This shift can be explained simply by the fact that upon initial binding of CB7 to the Ad

moiety, CB6 is (before slipping-off) pushed closer to the IB end. The isobutyl moiety is thus closer to the CB6's portals, resulting in the deshielding of corresponding H-atoms (state B, red). Subsequently, a new set of signals appears at a significantly higher field, indicating the release of CB6 from this 'metastable' complex **R2**@CB7^{Ad} to the IB binding site (state C, blue). Figure 17 (**2**) than shows kinetics curves for all three states (A, B and C) involved in the decomposition of the rotaxane **R2**.

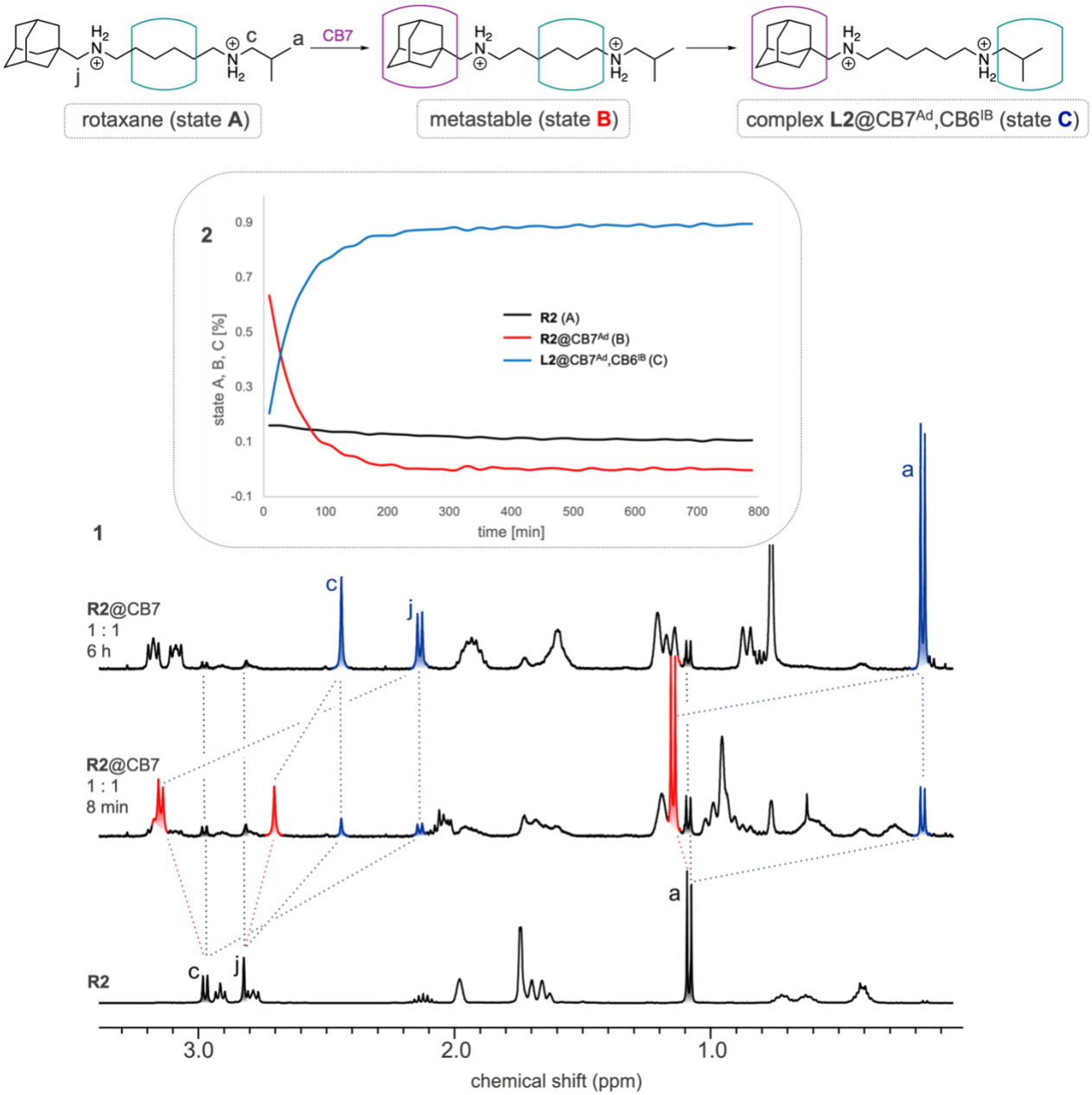

Figure 17 ^{1}H NMR spectra from the kinetics experiment of **R2** (0.85 mM) dethreading process at 303 K (**1**); portions of A, B and C forms of the **R2**+CB7 system in time at 303 K (**2**).

Subsequently, we repeated the kinetic measurements with different ratios of CB7 (0.5, 1.0, 1.5 and 2.0 equivalents) and rotaxane **R2**. From Figure 18, it can

be seen that in the presence of an excess of CB7, there is complete decomposition of a rotaxane. Conversely, with 0.5 equivalents, approximately 56% of the rotaxane remains in the system after 25 hours. The obtained data demonstrate that rate of the CB6 dethreading depends on the concentration of the **R2**@CB7 complex and is not affected by an excess of CB7. In other words, CB6 slipping off is a rate-determining step, while binding of CB7 at allosteric Ad site is significantly faster.

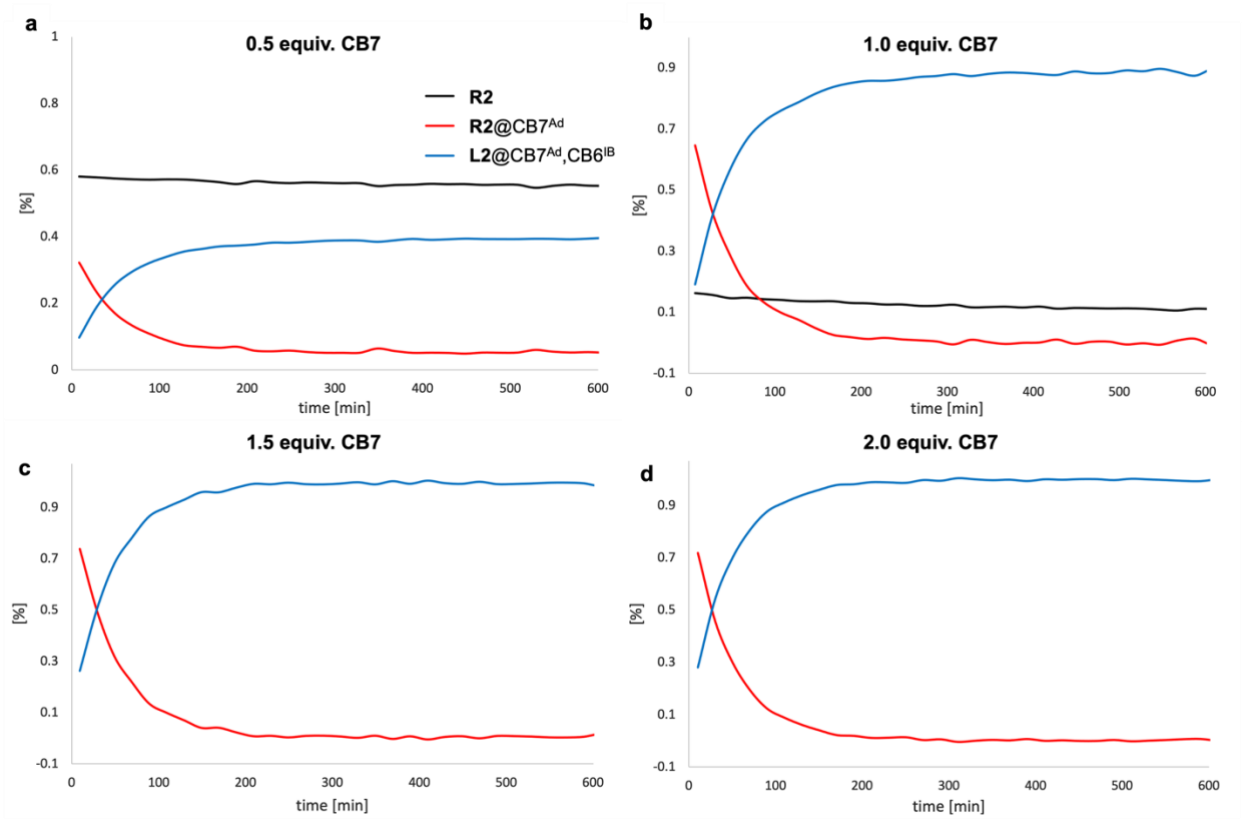

Figure 18 The kinetics curves for decomposition of **R2**@CB7 ($c_{\mathbf{R2}}$=0.83 mM) with various concentrations of CB7: (**a**) c_{CB7}=0.42 mM; (**b**) c_{CB7}=0.84 mM; (**c**) c_{CB7}=1.25 mM; (**d**) c_{CB7}=1.67 mM.

The behaviour of **R7**–**R10**@CB7 complexes was studied by heating them in D_2O at 353 K and monitoring changes over time using NMR. Rotaxanes **R7**–**R9** (ethylene, propylene, and allyl linker) showed gradual dethreading of CB6 at varying rates. In constrast, the aromatic rotaxane **R10** appeared thermodynamically stable, with no dethreading observed at this temperature. Kinetic experiments were conducted to determine the rate constants for rotaxanes dethreading (for **R2**: 283–303 K, for **R7**–**R10**: 333–353 K) using NMR to track their decomposition into **L**@CB6^{IB},CB7^{Ad} complexes. In Figure 19, kinetics curves illustrate decomposition of individual rotaxanes upon complexation with CB7 at various temperatures.

The kinetic data for **R**@CB7 decomposition followed a first-order model, allowing determination of dethreading rate constant *k* at various temperatures. Eyring plots provided energetic barriers for the slipping-off process, with results summarized in Table 2, including half-lives at 303 K. Notably, **R8** and **R9** showed half-lives od 1524 and 451 days, respectively. The shorter double bond in **R9** likely increases repulsion between CB6 and CB7 portals, accelerating dethreading compared to **R8**.

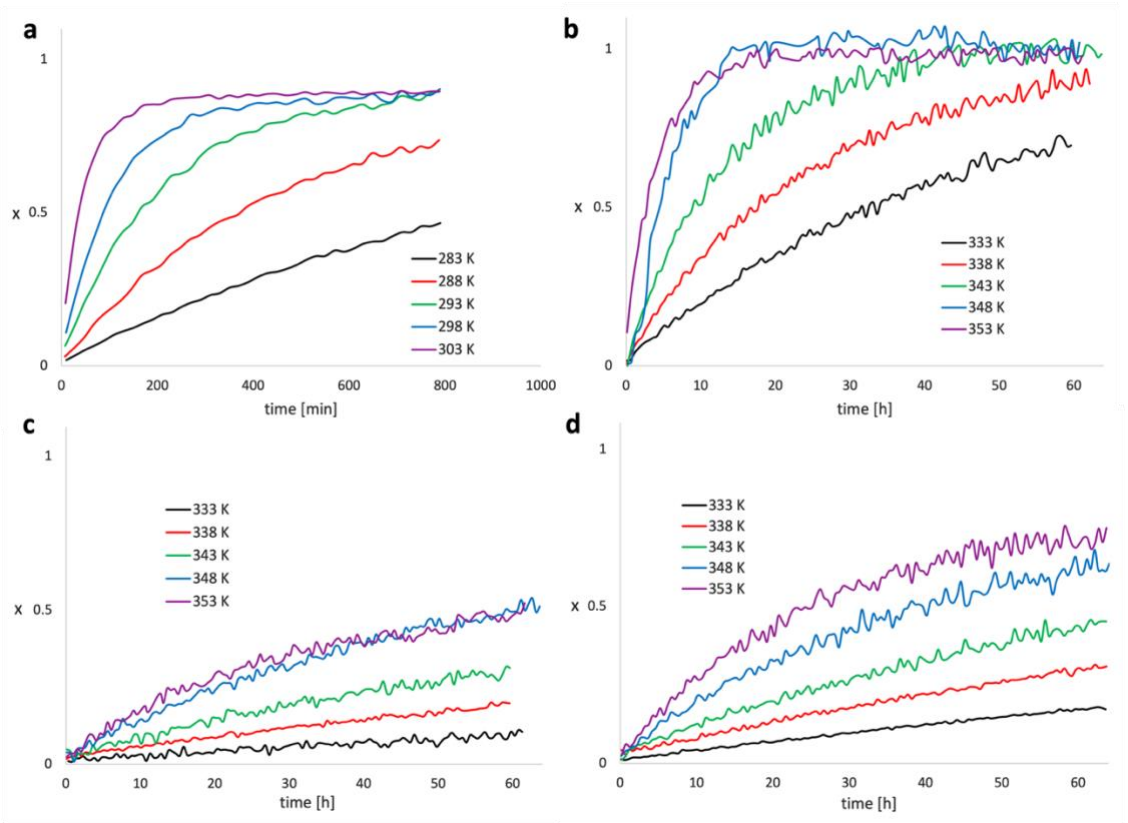

Figure 19 The kinetic curves for decomposition of **R2** (**a**) and **R7–R9** (**b**–**d**) complexes with CB7 at various temperatures.

Table 2 Kinetic parameters of CB6 slipping-off process.

guest	$\Delta G^{\ddagger}$(303 K)[a] [kJ·mol^{-1}]	$\Delta H^{\ddagger}$ [a] [kJ·mol^{-1}]	$\Delta S^{\ddagger}$[a] [J·mol^{-1}·K^{-1}]	$t_{1/2}$ (303 K)[b]
R2	94.5	104.9	34.2	36 min
R7	117.2	134.8	58.1	204 d
R8	122.3	121.8	−1.6	1524 d
R9	119.2	105.1	−46.4	451 d
R10	≥130[c]	na	na	∞

[a] Calculated from Eyring plots, [b] extrapolated from Eyring plots, [c] estimated (as Masson published, the kinetic barrier for slipping-on process is 121 kJ·mol^{-1}, thus we suppose that the barrier for the inverse process must be higher; in other words, the distribution of CB6 in case of **R10** is not affected by the presence of CB7). Na = not applicable.

We tested whether CB6 could be released from the aromatic **R10** under extreme conditions by heating its CB7 complex to 393 K for 2 hours (slipping-on conditions). The results showed that CB7 occupying the 4-(1-adamantyl)benzyl moiety has an insignificant impact on CB6 within the rotaxane, and the complex **R10**@CB7^{Ad} is thermodynamically preferred arrangement even at 393 K (see Figure 20). This fact implies that we have successfully identified two edge situations (rapid dethreading of the CB6 upon the CB7 signal at room temperature for **R2** and essentially no dethreading at 393 K for **R10**) in this series of molecular switches that respond to a combination of chemical and thermal stimuli.

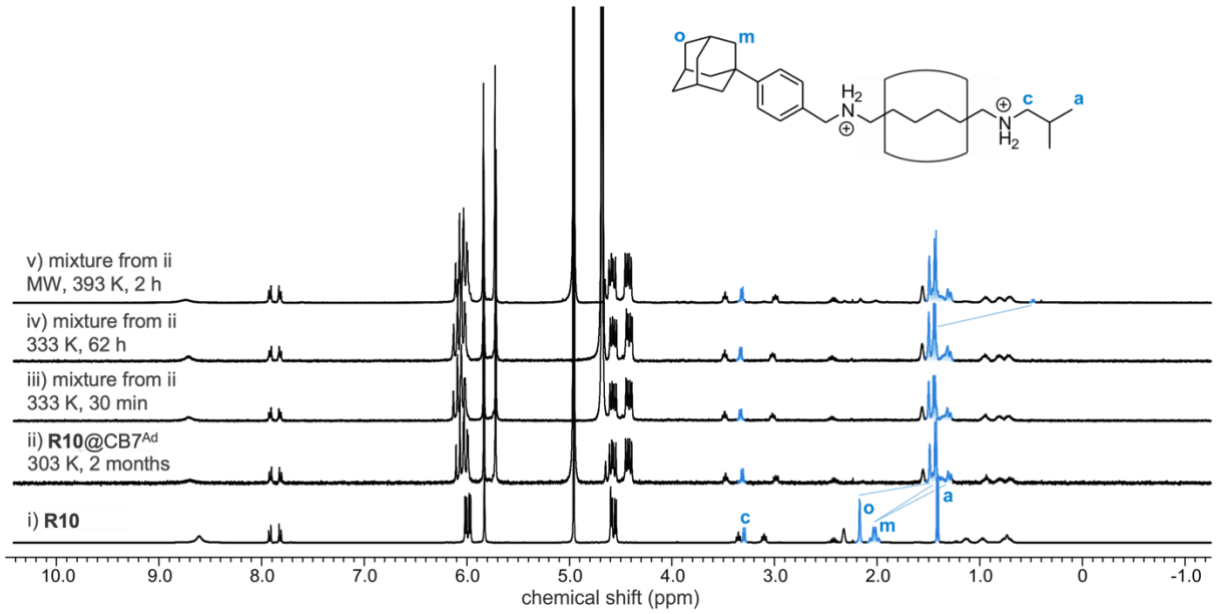

Figure 20 ^{1}H NMR spectra recorded during the experiments performed on rotaxane **R10** with CB7.

4.5 Releasing of CB6 to form other complexes

We investigated whether CB6, released from rotaxanes upon CB7 complexation, could be available for additional guests like spermine (SP) in the solution. First we prepare equimolar mixture of **R2** (0.68 mM) and SP. Subsequently, we added 1 equivalent of CB7 and monitored the progress by ^{1}H NMR. Immediately after the CB7 addition, the complex SP@CB7 was formed almost quantitatively (with respect to CB7). Subsequently, CB7 slowly moved to the Ad site following the termodynamical preference. CB7 at Ad site initiated the dethreading of CB6 and its binding to the SP.

The spectra illustrating this reorganization process are shown in Figure 21, Signals assignment for the last spectrum (line iv) was performed using TOCSY NMR analysis.

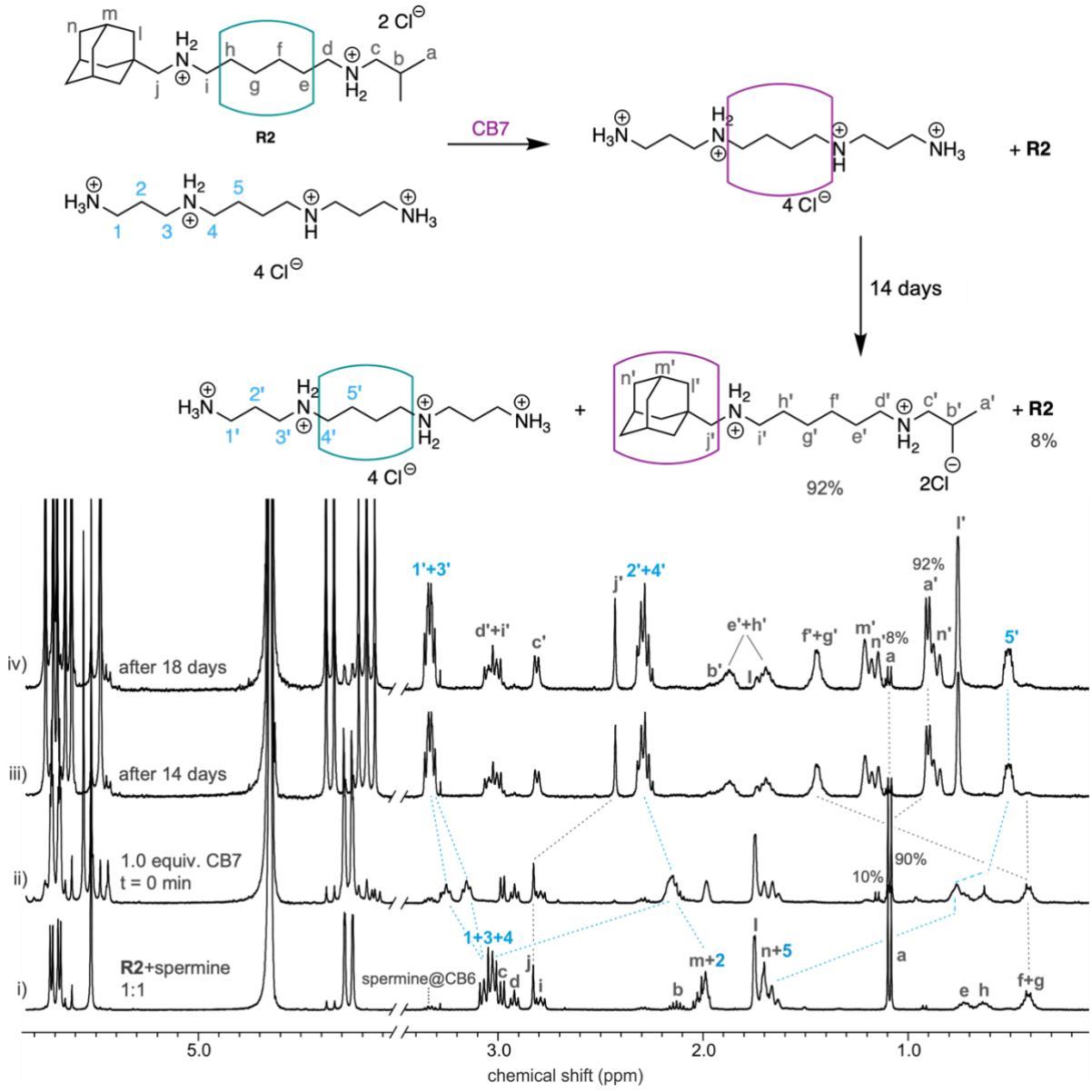

Figure 21 Competitive binding experiment of **R2** (0.68 mM) and SP with CB7 (1:1:1) at 303 K.

4.6 Association constants with β-CD, CB6 and CB7

K determination of ligands/rotaxanes complexes with β-CD using ITC

The binding behaviour of β-CD complexes with ligands and rotaxanes was described above using NMR titrations. The formation of complexes with a 1:1 stoichiometry where β-CD binds at the Ad site was expected, so the results were unsurprising. What primarily interested us was the comparison of binding constants between ligands and their corresponding rotaxanes with β-CD. In other words, how CB6 interlocked within the rotaxane would affect the binding strength of β-CD at the Ad moiety. The results of the ITC measurements are summarised

and compared in Table 3 (all measurements were performed only once due to the time constraints).

Table 3 ITC results for the **L**/**R**@β-CD^{Ad} complexes in distilled water at 303 K.

guest	n	K [M^{-1}]	ΔH [kJ·mol^{-1}]	ΔS [J·mol^{-1}·K^{-1}]	ΔG [kJ·mol^{-1}]
L2	0.987	2.65×10^4	−25.36	1.06	−25.67
R2	0.835	9.20×10^4	−36.83	−26.38	−28.81
L7	0.956	1.71×10^5	−32.32	−6.36	−30.37
R7	0.904	1.83×10^5	−34.81	−14.03	−30.64
L8	0.988	3.64×10^5	−33.58	−4.23	−32.27
R8	0.850	4.88×10^5	−36.93	−12.85	−33.01
L9	0.997	3.46×10^5	−33.24	−3.54	−32.15
R9	0.842	3.86×10^5	−36.69	−14.03	−32.42
L10	1.120	1.08×10^6	−35.28	−0.81	−35.01
R10	0.753	1.99×10^6	−46.98	−34.29	−36.55

Several interesting points can be observed in the Table 3. The first one is that prolonging the linker between the Ad cage and the ammonium moiety increases the values of *K*. The difference between adamantylmethylammonium (**L2**/**R2**) and the adamantylbenzylammonium (**L10**/**R10**) is hundredfold. This phenomenon can be explained by the fact that, given the volume of the β-CD's cavity (262 Å)[63] and Ad itself (159 Å),[64] structures with longer hydrophobic chains at the Ad can fit better into the cavity. This could then lead to stronger disperse interactions. Secondly, the difference in binding constants between the individual ligands and their corresponding rotaxanes is significant only in case of **L2**/**R2**. This implies that in this case, the portals of CB6 and β-CD are in close proximity, and so the hydrogen bonds formed between them contribute to the stability of β-CD on the Ad site. In other cases, the distance between the macrocycles is already relatively large, leading to minimal differences in binding constants between ligands and rotaxanes with β-CD.

Determination of *K* for complexes of ligands with CB6 by NMR

Due to the unclear results from the ITC analyses, we decided to determine the association constants for **L**@CB6 using a competitive ^{1}H NMR as an alternative

method. Thus, we mixed equimolar amounts of the corresponding ligand **L**, competitor (HMDA, $K_{HMDA@CB6} = 2.9\times10^8\ M^{-1}$, by ITC in 50 mM NaCl) and CB6 in 50 mM NaCl and let the mixtures equilibrate over the weekend at ambient temperature. Subsequently, we measured the ^{1}H NMR spectra, and identified the crucial signals corresponding to the free/complexed ligand and free/complexed competitor. By integrating these signals and considering the exact concentrations of ligand/competitor, we calculated the association constants according to the equation provided below. Figure 22 represents an example of the competitive experiment for mixture **L2**@CB6. For results see Table 4.

$$K_a = \frac{[\mathbf{L}@\mathrm{CB6}]\cdot[\mathrm{C}]_{\mathrm{free}}}{[\mathrm{C}@\mathrm{CB6}]\cdot[\mathbf{L}]_{\mathrm{free}}}\cdot K_a(\mathrm{C})$$

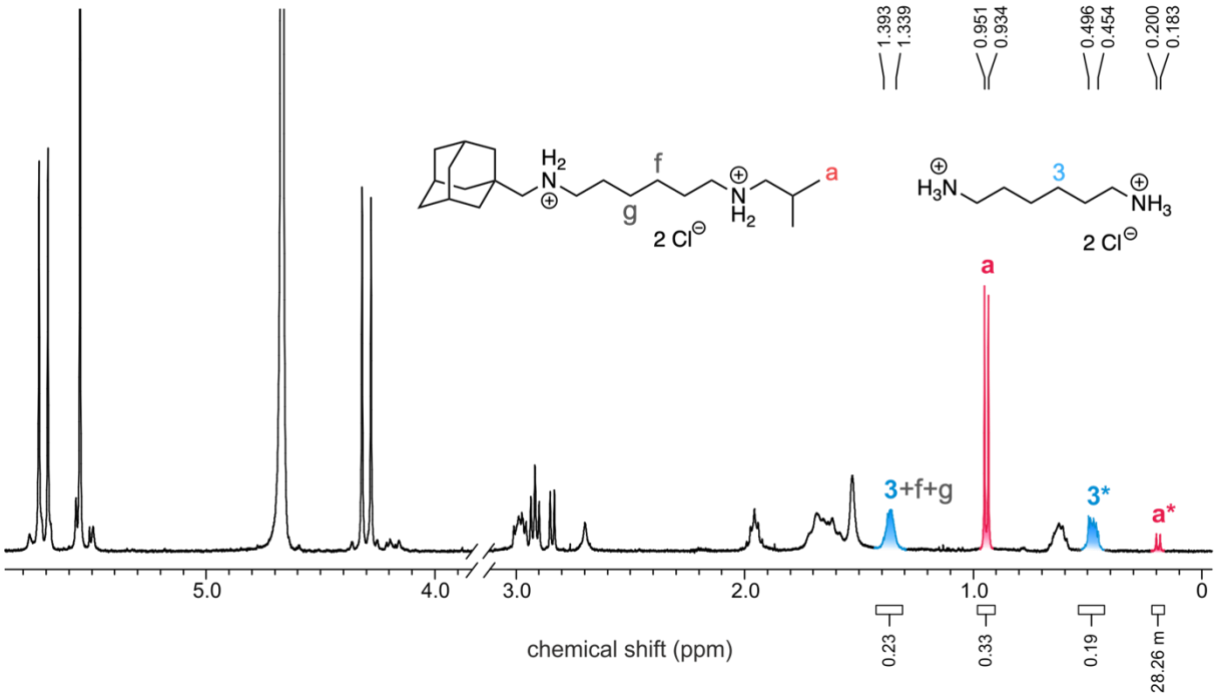

Figure 22 ^{1}H NMR spectrum of competitive binding experiment for **L2**@CB6 (competitor: HMDA) in 50 mM NaCl at 303 K. The key signals are highlighted for clarity. Signals associated with complexed components are marked with an asterisk.

Determination of *K* for complexes of ligands/rotaxanes with CB7 by NMR

We also performed competitive binding experiments using ^{1}H NMR to determine the association constants for **L**/**R** with CB7. Due to the presence of multiple binding sites on ligands, it was challenging. However, with a suitable competitor, we found that CB7 predominantly binds to the Ad site while ignoring the IB site, allowing us to treat the ligands as having a single binding site, and to determine the *K*. For rotaxanes, CB7 binds only to Ad site, as was described

earlier, simplifying the process. Unfortunately, we could not determine the constant for **R2** due to the rapid CB6 release upon complexation with CB7. For other rotaxanes, the constants were calculated using the same equation as described above. For results see Table 4.

Table 4 *K* for L/R@CB6/CB7 determined by competitive ^{1}H NMR experiments.

guest	@CB6 *K* [M^{-1}][a]	@CB7 *K* [M^{-1}] [b] (c)
L2	$2.5 \pm 0.1\times10^6$	$2.11 \pm 0.43\times10^{13}$ (AMMI)
R2	na	na
L7	$2.3 \pm 0.2\times10^6$	$9.73 \pm 0.20\times10^{11}$ (AMMI)
R7	na	$6.94 \pm 0.15\times10^9$ (PXD)
L8	$2.5 \pm 0.3\times10^6$	$3.39 \pm 0.58\times10^{11}$ (AMMI)
R8	na	$5.66 \pm 0.59\times10^{10}$ (PXD)
L9	$2.4 \pm 0.1\times10^6$	$1.44 \pm 0.05\times10^{11}$ (AMMI)
R9	na	$4.03 \pm 0.39\times10^{10}$ (PXD)
L10	$2.7 \pm 0.1\times10^6$	$1.81 \pm 0.15\times10^{11}$ (PXD)
R10	na	$1.04 \pm 0.03\times10^{10}$ (PXD)

[a] 50 mM NaCl, 303 K, HMDA as a competitor (c); [b] D_2O, 303 K, (c) AMMI = 1-(1-adamantylmethyl)-3-methylimidazolium iodide, PXD = *p*-xylylenediammonium chloride; na = not applicable

It is evident that with the increasing length between the Ad cage and the positively charged nitrogen atom, the differences in binding affinities between the axle and its rotaxane towards CB7 decreases. For **L7**/**R7** the difference is approximately 140:1, while for the aromatic **L10**/**R10** it is only 17:1. The explanation lies in the interactions between the macrocycles portals. In the complexes of L/R with CB6 and CB7, repulsions occur between the carbonyl portals. Naturally, the closer the macrocycles are to each other, the more strongly they are repulsed. In contrast, complexes with β-CD involve attractions due to the hydrogen bonds formation.

CONCLUSION

The main idea of this doctoral thesis was to design and prepare a molecular probe for the quantification of portal–portal repulsions/attractions. For this purpose, rotaxane structures with subtle structural variations were designed, synthesised, and their supramolecular behaviour was investigated. The aim was to explore the interactions between the macrocycle interlocked within the rotaxane manner and the additional bound macrocyclic unit.

The original concept behind our rotaxanes desing was to vary the length of the central carbon chain (C = 4, 6, 8, 10) as the binding motif for CB6, while the axel termini remain the same. This approach allows for the measurement of CB6 displacement along the variable-length central parts, thereby enabling the determination of the degree of repulsion (with CB7) or attraction (with β-CD). One of the axel termini is the IB motif, allowing for CB6 to slips on at 393 K, with a kinetic barrier of 121 kJ·mol^{-1}.[39] The second is the adamantylmethyl end serving as an ultimate stopper for CB6 and simultaneously as a strong binding site for CB7 or β-CD. These four ligands (**L1**–**L4**), which act as the axel components for the envisioned rotaxanes, represent the **first-generation** of ligands in this work. However, only the ligand with hexyl linker **L2** achieved high rotaxane **R2** formation (91%) under synthesis conditions, as equilibrium reaction favoured interlocked structure. Shorter or longer ligands shower reduced efficiency due to weaker binding and unavourable equilibrium, with **R1**/**R3**/**R4** yielding minimal or no rotaxane formation.

Continuing the supramolecular studies on the rotaxane **R2** with CB7, we discovered, to our surprise, that the binding of CB7 at the Ad terminus iniciate the CB6 slipping-off process from the rotaxane. In other words, the repulsions between the carbonyl portals of the macrocycles forced CB6 to slip off from the so far kinetically stable rotaxane. Thus, we decided to increase the energetic barrier on the CB6-threading stopper to prepare **second-generation** ligands (**L5**, **L6**), and waited to see if CB6 would or would not slip off upon binding CB7. We replaced the isobutyl stopper for the neopentyl-derived motif. Nevertheless, the barrier was so high, that even the initial complex **L**@CB6 was not formed at 303 K, and none of the methods used (MW, 393 or 423 K, 2–4 h) for rotaxane preparation were successful.

For this reason, we moved with the structure modification to the opposite terminus of the original ligand **L2** and increased the length of the linker between the Ad and positively charged nitrogen atom to prepare **third-generation** ligands (ethan-1,2-diyl **L7**, propan-1,3-diyl **L8**, propen-1,3-diyl **L9** and 4-(1-adamantyl)benzyl linker **L10**). Since these ligands bear the IB terminal moiety and HMDA centrepiece, the formation of the respective rotaxanes **R7**–**R10** was successful. Subsequently, a purification method was developed using liquid

chromatography with a H_2O/MeCN/HCOOH (5/2/1, v/v/v) mobile phase. The rotaxane structures were confirmed by 1D and 2D NMR and ESI-MS analysis. We also succeeded in growing single crystals of **R2** and **R7**–**R9**, and X-ray diffraction analysis confirmed the positioning of the CB6 unit at the HMDA binding site

Before examining the supramolecular properties of the rotaxanes, it was essential to first test and confirm their stability in an aqueous media using competitors 1,6-hexamethylendiamine (HMDA) and spermine (SP). We mixed equimolar amounts of **R2** with HMDA/SP and monitored these mixtures by ^{1}H NMR. Since no changes in the spectra were observed within three months, the rotaxanes were considered kinetically stable at 303 K. Additionally, we added into these mixtures one equivalent of CB7. CB6, once released from the rotaxane, was shown to be available for other guests with higher affinity, such as HMDA or SP ($K = 2.9\times10^8$ M^{-1} or 3.3×10^9 M^{-1}, respectively; ITC, 50 mM NaCl, 298 K). The formation of **L**@CB7^{Ad} and HMDA/SP@CB6 complexes was confirmed by ^{1}H NMR (TOCSY analyses were used for signals assignment).

Once we confirmed the long-term stability of the rotaxanes, we could continue with supramolecular studies with CB7 to investigate how the length of the allosteric binding site influences the CB6 slipping off. Binding with CB7 at 303 K suggests that CB7 binds to the high affinity adamantane motif. Since no other shifts of the signals occurred within 2 months, the complexes **R7**–**R10**@CB7^{Ad} were considered stable at room temperature. We then treated these mixtures at elevated temperature (333 K) and monitored the CB6-slipping off as a result of repulsive interaction between macrocycles (for **R7**–**R9**). The CB7 unit occupying the longest adamantylbenzyl motif (**R10**) had insignificant impact on CB6 within the rotaxane and the complex **R10**@CB7^{Ad} was thermodynamically preferred arrangement, even at 393 K (conditions of rotaxane formation). We subsequently determined the rate constants for the dethreading processes by kinetics experiments using ^{1}H NMR at various temperatures. From obtained data, we constructed an Eyring plots and calculated the energetic bariers along with half-lives for the **R**@CB7^{Ad} (**R2**: $\Delta G^{\ddagger} = 94.5$ kJ·mol^{-1}, $\tau_{1/2} = 36$ min; **R7**: $\Delta G^{\ddagger} = 117.2$ kJ·mol^{-1}, $\tau_{1/2} = 204$ days; **R8**: $\Delta G^{\ddagger} = 122.4$ kJ·mol^{-1}, $\tau_{1/2} = 1524$ days and **R9**: $\Delta G^{\ddagger} = 119.2$ kJ·mol^{-1}, $\tau_{1/2} = 451$ days).

In addition, we determined the thermodynamic parameters and binding constants for ligands with β-CD (using ITC), CB6 and CB7 (using NMR). ITC results confirmed the 1:1 stoichiometry in all examined complexes (β-CD sits on the Ad bindining site). It was found that as the length of the linker between the Ad cage and the ammonium moiety increases, the values of the association constant increase as well ($K = 2.7–200\times10^4$ M^{-1}). The difference in binding constants between the individual ligands and their corresponding rotaxanes is significant only in case of **L2**/**R2** (**L2**: 2.7×10^4, **R2**: 9.2×10^4). This suggest that in

this case, the portals of CB6 and β-CD are in close proximity, and so the hydrogen bonds formed between them contribute to the stability of β-CD on the adamantane site. In other cases, the distance between the macrocycles is relatively large, leading to minimal differences in binding constants between ligands and rotaxanes with β-CD. Complexes with CB6 are formed only in the case of ligands **L**. Due to the electrostatic repulsive interactions, there is not enough space for another CB6 on rotaxanes at IB end. In addition, CB6 is too small to form an inclusion complexes with the Ad cage. We measured the association constants for **L**@CB6 complexes using NMR with the HMDA as a competitor. The *K* values were consistently around 2.5×10^{6} M^{-1}. Mixtures of rotaxanes with CB7 required several days long equilibration, making the use of ITC impossible to determine the binding constants, thus we used the ^{1}H NMR competitive experiment with *p*-xylylenediamine or 1-(1-adamantylmethyl)-3-methylimidazolium bromide as competitors. The results suggest that the differences in *K* values between the ligands and their respective rotaxanes with CB7 decreases with the increasing length of the linker. For **L7**/**R7** (9.7×10^{11} / 6.9×10^{9}), the difference is slightly over two orders of magnitude, while for the aromatic **L10**/**R10** (1.8×10^{11} / 1.0×10^{10}), it is only one order of magnitude. The explanation lies again in the interactions between the macrocycles portals. While in **L**/**R**@β-CD^{Ad} complexes, hydrogen bonds formed between CB6 and β-CD result in attraction, portal–portal interactions between CB6 and CB7 in **L**/**R**@CB7^{Ad} complexes lead to repulsion. The closer the macrocycles are to each other, the more strongly they are repulsed.

In conclusion, it is important to highlight that this work introduces a novel methodology for transitioning a static and kinetically stable CB6-based rotaxane system to a dynamic state, resulting in the dethreading of the wheel. These findings are particularly significant considering the high selectivity and large range of association constants of cucurbit[*n*]urils, which makes them promising components of molecular devices, for example molecular memories, catalysts or drug delivery systems.

The next step for my successors would be to incorporate and utilize the CB6 releasing trigger within more complex supramolecular systems, either in multicomponent mixtures or in an intramolecular manner.

REFERENCE

[1] Lehn, J.-M. From Matter to Life: Chemistry?!. *Reson.* **1996**, *1*, 39–53. online

[2] Deutman, A. B. C.; Cantekin, S.; Elemans, J. A. A. W.; Rowan, A. E.; Nolte, R. J. M. Designing Processive Catalytic Systems. Threading Polymers through a Flexible Macrocycle Ring. *J. Am. Chem. Soc.* **2014**, *136*, 9165–9172. online

[3] David, A. H. G.; García-Cerezo, P.; Campaña, A. G.; Santoyo-González, F.; Blanco, V. Vinyl sulfonyl chemistry-driven unidirectional transport of a macrocycle through a [2]rotaxane. *Org. Chem. Front.* **2022**, *9*, 633–642. online

[4] Tamura, A.; Yui, N. Rational design of stimuli-cleavable polyrotaxanes for therapeutic applications. *Polym. J.* **2017**, *49*, 527–534. online

[5] Slack, C. C.; Finbloom, J. A.; Jeong, K.; Bruns, C. J.; Wemmer, D. E.; Pines, A.; Francis, M. B. Rotaxane probes for protease detection by ^{129}Xe hyperCEST NMR. *Chem. Commun.* **2017**, *53*, 1076–1079. online

[6] Kench, T.; Summers, P. A.; Kuimova, M.; Lewis, J. E. M.; Vilar, R. Rotaxanes as Cages to Control DNA Binding Cytotoxicity, and Cellular Uptake of a Small Molecule. *Angew. Chem. Int. Ed.* **2021**, *60*, 10928–10934. online

[7] Guo, Q.-H.; Qui, Y.; Kuang, X.; Liang, J.; Feng, Y.; Zhang, L.; Jiao, Y.; Shen, D.; Astumian, R. D.; Stoddart, J. F. Artificial Molecular Pump Operating in Response to Electricity and Light. *J. Am. Chem. Soc.* **2020**, *142*, 14443–14449. online

[8] Li, X.; David, A. H. G.; Zhang, L.; Song, B.; Jiao, Y.; Sluysmans, D.; Qui, Y.; Wu, Y.; Zhao, X.; Feng, Y.; Mosca, L.; Stoddart, J. F. Fluorescence Quenching by Redox Molecular Pumping. *J. Am. Chem. Soc.* **2022**, *144*, 3572–3579. online

[9] Ren, Y.; Jamagne, R.; Tetlow, D. J.; Leigh, D. A. A tape-reading molecular rachet. *Nature* **2022**, *612*, 78–82. online

[10] Thomas, D.; Tetlow, D. J.; Ren, Y.; Kassem, S.; Karaca, U.; Leigh, D. A. Pumping between phases with a pulsed-fuel molecular rachet. *Nat. Nanotechnol.* **2022**, *17*, 701–707. online

[11] Muramatsu, T.; Okado, Y.; Traeger, H.; Schrettl, S.; Tamaoki, N.; Weder, Ch.; Sagara, Y. Rotaxane-Based Dual Function Mechanophores Exhibiting Reversible and Irreversible Responses. *J. Am. Chem. Soc.* **2021**, *143*, 9884–9892. online

[12] Leigh, D. A.; Pirvu, L.; Schaufelberger, F.; Tetlow, D. J.; Zhang, L. Securing a Supramolecular Architecture by Tying a Stopper Knot. *Angew. Chem. Int. Ed.* **2018**, *57*, 10484–10488. online

[13] Zhang, K.-D.; Zhao, X.; Wang, G.-T.; Liu, Y.; Zhang, Y.; Lu, H.-J.; Jiang, X.-K.; Li, Z.-T. Foldamer–tuned switching kinetics and metastability of [2]rotaxanes. *Angew. Chem. Int. Ed.* **2011**, *50*, 9866–9870. online

[14] Rajappan, S. C.; McCarthy, D. R.; Campbell, J. P.; Ferrell, J. B.; Sharafi, M.; Ambrozaite, O.; Li, J.; Schneebeli, S. T. Selective Monofunctionalization Enabled by Reaction-History-Dependent Communication in Catalytic Rotaxanes. *Angew. Chem. Int. Ed.* **2020**, *59*, 16668–16674. online

[15] Zhang, M.; Bo, G. D. Mechanical Susceptibility of a Rotaxane. *J. Am. Chem. Soc.* **2019**, *141*, 15879–15883. online

[16] Saura-Sanmartin, A. Light-responsive rotaxane-based materials: inducing motio in the solid state. *Beilstein. J. Org. Chem.* **2023**, *19*, 873–880. online

[17] Arisaka, Y.; Yui, N. Suspending Polyrotaxane Dissociation via Photo-Reversible Capping of Terminals. *Macromol. Rapid. Commun.* **2019**, *40*, 1900323. online

[18] Feng, L.; Qui, Y.; Guo, Q.-H.; Chen, Z.; Seale, J. S. W.; He, K.; Wu, H.; Feng, Y.; Farha, O. K.; Astumian, R. D.; Stoddart, J. F. Active mechanisorption driven by pumping cassettes. *Science* **2021**, *374*, 1215–1221. online
[19] Dongen, S. F. M. van; Cantekin, S.; Elemans, J. A. A. W.; Rowan, A. E.; Nolte, R. J. M. Functional interlocked systems. *Chem. Soc. Rev.* **2014**, *43*, 99–122. online
[20] Neal, E. A.; Goldup, S. M. Chemical consequences of mechanical bonding in catenanes and rotaxanes: isomerism, modification, catalysis and molecular machines for synthesis. *Chem. Commun.* **2014**, *50*, 5128–5142. online
[21] Ashton, P. R.; Johnston, M. R.; Stoddart, J. F.; Tolley, M. S.; Wheeler, J. W. The Template-directed Synthesis of Porphyrin-stoppered [2]Rotaxanes. *J. Chem. Soc., Chem. Commun.* **1992**, 1128–1131. online
[22] Askawa, M.; Ashton, P. R.; Iqbal, S.; Quick, A.; Stoddart, J. F.; Tinker, N. D.; White, A. J. P.; Williams, D. J. Functionalized [2]rotaxanes. *Isr. J. Chem.* **1997**, *36*, 329–340. online
[23] Glink, P. T.; Oliva, A. I.; Stoddart, J. F.; White, A. J. P.; Williams, D. J. Template-Directed Synthesis of a [2]Rotaxane by the Clipping under Thermodynamic Control of a Crown Ether Like Macrocycle Around a Dialkylammonium Ion. *Angew. Chem.* **2001**, *113*, 1922–1927. online
[24] Rao, T. V. S.; Lawrence, D. S. Self-Assembly of a Threaded Molecular Loop. *J. Am. Chem. Soc.* **1990**, *112*, 3614–3615. online
[25] Reuter, C.; Wienand, W.; Hübner, G. M.; Seel, Ch.; Vögtle, F. High-Yield Synthesis of Ester, Carbonate, and Acetal Rotaxanes by Anion Template Assistance and Their Hydrolytic Dethreading. *Chem. Eur. J.* **1999**, *5*, 2692–2697. online
[26] Isnin, R.; Kaifer, A. E. Novel Class of Asymmetric Zwitterionic Rotaxanes Based on α-Cyclodextrin. *J. Am. Chem. Soc.* **1991**, *113*, 8188–8190. online
[27] Crowley, J. D.; Goldup, S. M.; Lee, A.-L.; Leigh, D. A.; McBurney, R. T. Active metal template synthesis of rotaxanes, catenanes and molecular shuttles. *Chem. Soc. Rev.* **2009**, *38*, 1530–1541. online
[28] Qu, D.-H.; Tian, H. Novel and efficient templates for assembly of rotaxanes and catenanes. *Chem. Sci.* **2011**, *2*, 1011–1015. online
[29] Beves, J. E.; Blight, B. A.; Campbell, Ch. J.; Leigh, D. A.; McBurney, R. T. Strategies and Tactics for the Metal-Directed Synthesis of Rotaxanes, Knots, Catenanes, and Higher Order Links. *Angew. Chem. Int. Ed.* **2011**, *50*, 9260–9327. online
[30] Ashton, P. R.; Bělohradský, M.; Philp, D.; Stoddart, J. F. Slippage – and Alternative Method for assembling [2]Rotaxanes. *J. Chem. Soc., Chem. Commun.* **1993**, 1269–1274. online
[31] Ashton, P. R.; Bělohradský, M.; Philp, D.; Spencer, N.; Stoddart, J. F. The Self Assembly of [2]- and [3]-Rotaxanes by Slippage. *J. Chem. Soc., Chem. Commun.* **1993**, 1274–1277. online
[32] Asakawa, M.; Ashton, P. R.; Ballardini, R.; Balzani, V.; Bělohradský, M.; Gandolfi, M. T.; Kocian, O.; Prodi, L.; Raymo, F. M.; Stoddart, J. F.; Venturi, M. The Slipping Approach to Self-Assembling [*n*]Rotaxanes. *J. Am. Chem. Soc.* **1997**, *119*, 302–310. online
[33] Yoon, I.; Narita, M.; Shimizu, T.; Asakawa, M. Threading-Followed-by-Shrinking Protocol for the Synthesis of a [2]Rotaxane Incorporating a Pd(II) – Salophen Moiety. *J. Am. Chem. Soc.* **2004**, *126*, 16740–16741. online
[34] Hsueh, S.-Y.; Ko, J.-L.; Lai, Ch.-Ch.; Liu, Y.-H.; Peng, S.-M.; Chiu, S.-H. A Metal Free "Threading-Followed-by-Shrinking" Protocol for Rotaxane Synthesis. *Angew. Chem. Int. Ed.* **2011**, *50*, 6643–6646. online
[35] Chiu, Ch.-W.; Lai, Ch.-Ch.; Chiu, S.-H. "Threading-Followed-by-Swelling": A New Protocol for Rotaxane Synthesis. *J. Am. Chem. Soc.* **2007**, *129*, 3500–3501. online
[36] Fujimura, K.; Ueda, Y.; Yamaoka, Y.; Takasu, K.; Kawabata, T. Rotaxane Synthesis by an End-Capping Strategy via Swelling Axle-Phenols. *Angew. Chem. Int. Ed.* **2023**, *62*, e202303078. online

[37] McConnell, A. J.; Beer, P. D. Kinetic Studies Exploring the Role of Anion Templation in the Slippage Formation of Rotaxane-Like Structures. *Chem. Eur. J.* **2011**, *17*, 2724–2733. online
[38] Masai, H.; Terao, J.; Fujihara, T.; Tsuji, Y. Rational Design for Rotaxane Synthesis through Intramolecular Slippage: Control of Activation Energy by Rigid Axle Length. *Chem. Eur. J.* **2016**, *22*, 6624–6630. online
[39] Ling, X.; Samuel, E. L.; Patchell, D. L.; Masson, E. Cucurbituril Slippage: Translation is a Complex Motion. *Org. Lett.* **2010**, *12*, 2730–2733. online
[40] Rekharsky, M. V.; Ko, Y. H.; Selvapalam, N.; Kim, K.; Inoue, Y. Complexation Thermodynamics of Cucurbit[6]uril with Aliphatic Alcohols, Amines and Diamines. *Supramol. Chem.* **2007**, *19*, 39–46. online
[41] Sun, H.-L.; Zhang, H.-Y.; Dai, Z.; Han, X.; Liu, Y. Insights into the Difference Between Rotaxane and Pseudorotaxane. *Chem. Asian. J.* **2017**, *12*, 265–270. online
[42] Ashton, P. R.; Baxter, I.; Fyfe, M. C. T.; Raymo, F. M.; Spencer, N.; Stoddart, J. F.; White, A. J. P.; Williams, D. J. Rotaxane or Pseudorotaxane? That Is the Question! *J. Am. Chem. Soc.* **1998**, *120*, 2297–2307. online
[43] Affeld, A.; Hübner, G. M.; Seel, Ch.; Schalley, Ch. A. Rotaxane or Pseudorotaxane? Effect of Small Structural Variations on the Deslipping Kinetics of Rotaxanes with Stopper Groups of Intermediate Size. *Eur. J. Org. Chem.* **2001**, 2877–2890. online
[44] Chiu, S.-H.; Rowan, S. J.; Cantrill, S. J.; Glink, P. T.; Garrell, R. L.; Stoddart, J. F. A Rotaxane-Like Complex with Controlled-Release Characteristics. *Org. Lett.* **2000**, *2*, 3631–3634. online
[45] Cherraben, S.; Scelle, J.; Hasenknopf, B.; Guillaume, V.; Sollogoub, M. Precise Rate Control of Pseudorotaxane Dethreading by pH-Responsive Selectively Functionalized Cyclodextrins. *Org. Lett.* **2021**, *23*, 7938–7942. online
[46] Fernandes, A.; Viterisi, A.; Coutrot, F.; Potok, S.; Leigh, D. A.; Aucagne, V.; Papot, S. Rotaxane-Based Propeptides: Protection and Enzymatic Release of a Bioactive Pentapeptide. *Angew. Chem. Int. Ed.* **2009**, *48*, 6443–6447. online
[47] D'Orchymont, F.; Holland, J. P. A rotaxane-based platform for tailoring the pharmacokinetics of cancer-targeted radiotracers. *Chem. Sci.* **2022**, *13*, 12713–12725. online
[48] Wu, P.; Dharmadhikari, B.; Patra, P.; Xiong, X. [2]Rotaxane as a switch for molecular electronic memory application: A molecular dynamics study. *J. Mol. Graph. Model.* **2022**, *114*, 108163. online
[49] Wu, P.; Dharmadhikari, B.; Patra, P.; Xiong, X. Rotaxane nanomachines in future molecular electronics. *Nanoscale Adv.* **2022**, *4*, 3418–3461. online
[50] Hertzog, J. E.; Maddi, V. J.; Hart, L. F.; Rawe, B. W.; Rauscher, P. M.; Herbert, K. M.; Bruckner, E. P.; Pablo, J. J. de; Rowan, S. J. Metastable doubly threaded [3]rotaxanes with a large macrocycle. *Chem. Sci.* **2022**, *13*, 5333–5344. online
[51] Sun, H.-L.; Zhang, H.-Y.; Dai, Z.; Han, X.; Liu, Y. Insights into the Difference Between Rotaxane and Pseudorotaxane. *Chem. Asian. J.* **2017**, *12*, 265–270. online
[52] Branná, P.; Rouchal, M.; Prucková, Z.; Dastychová, L.; Lenobel, R.; Pospíšil, T.; Maláč, K.; Vícha, R. Rotaxanes Capped with Host Molecules: Supramolecular Behavior of Adamantylated Bisimidazolium Salts Containing a Biphenyl Centerpiece. *Chem. Eur. J.* **2015**, *21*, 11712–11718. online
[53] Bissell, R. A.; Cordova, E.; Kaifer, A. E.; Stoddart, J. F. A chemically and electrochemically switchable molecular device. *Nature* **1994**, *369*, 133–137. online
[54] Blanco, V.; Carlone, A.; Hänni, K. D.; Leigh, D. A.; Lewandowski, B. A Rotaxane-Based Switchable Organocatalyst. *Angew. Chem.* **2012**, *124*, 5256–5259. online
[55] Badjić, J. D.; Balzani, V.; Credi, A.; Silvi, S.; Stoddart, J. F. A Molecular Elevator. *Science* **2004**, *303*, 1845–1849. online

[56] Zhu, L.; Yan, H.; Wang, X.-J.; Zhao, Y. Light-Controllable Cucurbit[7]uril-Based Molecular Shuttle. *J. Org. Chem.* **2012**, *77*, 10168–10175. online
[57] Gao, Ch.; Luan, Z.-L.; Zhang, Q.; Yang, S.; Rao, S.-J.; Qu, D.-H.; Tian, H. Triggering a [2]Rotaxane Molecular Shuttle by a Photochemical Bond-Cleavage Strategy. *Org. Lett.* **2017**, *19*, 1618–1621. online
[58] Barat, R.; Legigan, T.; Tranoy-Opalinski, I.; Renoux, B.; Péraudeau, E.; Clarhaut, J.; Poinot, P.; Fernandes, A. E.; Aucagne, V.; Leigh, D. A.; Papot, S. A mechanically interlocked molecular system programmed for the delivery of an anticancer drug. *Chem. Sci.* **2015**, *6*, 2608–2613. online
[59] Babjaková, E.; Branná, P.; Kuczyńska, M.; Rouchal, M.; Prucková, Z.; Dastychová, L.; Vícha, J.; Vícha, R. An adamantane-based disubstituted binding motif with picomolar dissociation constants for cucurbit[*n*]urils in water and related quarternary assemblies. *RSC Adv.* **2016**, *6*, 105146–105153. online
[60] Kulkarni, S. G.; Prucková, Z.; Rouchal, M.; Dastychová, L.; Vícha, R. Adamantylated trisimidazolium-based tritopic guests and their binding properties towards cucurbit[7]uril and β-cyclodextrin. *J. Incl. Phenom. Macrocycl. Chem.* **2016**, *84*, 11–20. online
[61] Branná, P.; Černochová, J.; Rouchal, M.; Kulhánek, P.; Babinský, M.; Marek, R.; Nečas, M.; Kuřitka, I.; Vícha, R. Cooperative Binding of Cucurbit[*n*]urils and β-Cyclodextrins to Heteroditopic Imidazolium-Based Guests. *J. Org. Chem.* **2016**, *81*, 9595–9604. online
[62] Kulkarni, S. G.; Jelínková, K.; Nečas, M.; Prucková, Z.; Rouchal, M.; Dastychová, L.; Kulhánek, P.; Vícha, R. A Photochemical/Thermal Switch Based on 4,4‘-Bis(benzimidazolio)stilbene: Synthesis and Supramolecular Properties. *ChemPhysChem.* **2020**, *21*, 2084–2095. online
[63] Szejtli, J. Utilization of cyclodextrins in industrial products and processes. *J. Mater. Chem.* **1997**, *7*, 575–587. online
[64] Jiménez-Cruz, F.; García-Gutiérrez, J. L. Molecular size and shape properties of diamondoid molecules occurring in crude oil. *Arab. J. Chem.* **2020**, *13*, 8592–8599. online

CURRICULUM VITAE

Academic curriculum vitae

Education

Ph.D. Technologie makromolekulárních látek
Tomas Bata University in Zlín
Doctoral Thesis: Synthesis of Rotaxane Structures with Multitopic Ligands

Ing. Chemie a technologie potravin (obor Chemie potravin a bioaktivních látek)
Tomas Bata University in Zlín
Master's Thesis: Synthesis and supramolecular properties of ligands based on adamantylacetylene

Bc. Chemie a technologie potravin (obor Technologie výroby tuků, kosmetiky a detergentů)
Tomas Bata University in Zlín
Bachelor's Thesis: Stanovení termodynamických parametrů komplexů cyklodextrinů s imidazoliovými solemi pomocí isotermální titrační mikrokalorimetrie

Abroad stays and internhips

University of Huelva, Spain **02–04/2022**
Photocontrol of dynamic chemical systems
Supervisor: Prof. Dr. Uwe Pischel

University of Science, Ho Chi Minh City, Vietnam **03–05/2018**
Freemover: Traineeship
Traineeship title: Laboratory experiments in natural products & medicinal chemistry

Instituto Politécnico de Beja, Portugal **02–06/2016**
Erasmus: Study internship

Publications

Jelínková. K.; Závodná, A.; Kaleta, J.; Janovský, P.; Zatloukal, F.; Nečas, M.; Prucková, Z.; Dastychová, L.; Rouchal, M.; Vícha, R. Two Squares in a Barrel: An Axially Disubstituted Conformationally Rigid Aliphatic Binding Motif for Cucurbit[6]uril. *J. Org. Chem.* **2023**, *88*, 15615–15626. online

Závodná, A.; Janovský, P.; Kolařík, V.; Ward, J. S.; Prucková, Z.; Rissanen, K.; Rouchal, M.; Vícha, R. Allosteric Release of Cucurbit[6]uril from a Rotaxane Using a Molecular Signal. *Chem. Sci.* **2024**, *early view*. online

Participation in grant projects

Internal Grant Agency in Zlín IGA/FT/2018/001 – Vysoce afinitní supramolekulární systémy, *spoluřešitel.*
Internal Grant Agency in Zlín IGA/FT/2019/007 – Příprava a studium vazebných motivů pro supramolekulární systémy, *spoluřešitel.*
Internal Grant Agency in Zlín IGA/FT/2020/001 – Studium intermolekulárních interakcí ve vícekomponentních systémech, *řešitel.*
Internal Grant Agency in Zlín IGA/FT/2021/001 – Multitopické ligandy: Od základních principů k funkčním molekulám, *spoluřešitel.*
Internal Grant Agency in Zlín IGA/FT/2022/001 – Rotaxanové katalyzátory, *spoluřešitel*.
Internal Grant Agency in Zlín IGA/FT/2023/001 – Supramolekulární stavebnice, *spoluřešitel*.

Project – Technology Agency CR (TA ČR) TJ04000226 – Kombinovaný postup eliminace chloracetanilidových pesticidů z kontaminovaných vod a zemin, *spoluřešitel*.

Conferences

A. Závodná, Z. Prucková, M. Rouchal, R. Vícha. Switching Rotaxane to Pseudorotaxane by Chemical Signals: A Crucial Role of Lateral Repulsive Interactions. CoNFeRenNCe Rosteme s chemií, 15.–16. 6. 2023, Pardubice.

Synthesis of Rotaxane Structures with Multitopic Ligands

Syntéza rotaxanových struktur s vícevazebnými ligandy

Doctoral Thesis Summary

Published by: Tomas Bata University in Zlín,

nám. T. G. Masaryka 5555, 760 01 Zlín.

Edition: published electronically

Typesetting by: Ing. Aneta Závodná, Ph.D.

This publication has not undergone any proofreading or editorial review.

Publication year: 2025

First Edition

ISBN 978-80-7678-323-2